

Aug. 15., 2016

Dear Editor,

Thank you for your comments and sorry for not including answers to them in the first round. We have followed your recommendations and given a reply to each of the two comments below.

Best regards Rasmus

Editor Decision: Publish subject to minor revisions (Editor review) (08 Jul 2016) by Dr. Christian Haas

Comments to the Author:

Dear Authors,

thank you for the revisions. However, I think you haven't addressed my comments from the initial Editor's review. Please could you consider to include my suggestions, and to reply to them. My comments:

1. Given that sea ice coverage trends have been published previously and extensively, and are well established since many years, the motivation for your work is not really clear. I understand that your work is significant because it introduces new time series based on new algorithms, which are potentially superior to previously published work. I also understand that you may want to avoid statements as to which products are better, which is hard to convincingly prove anyways. However, I would like to request that you at least include comparison between the trends derived by you with previously published trends, and what the possible reasons for the agreements or disagreements are. Only then can the consequences and impacts of your work be evaluated, and why it would be worthwhile to reconcile studies of Arctic and Antarctic sea ice trends with your new product.

Reply:

Thanks for pointing this out. It is indeed important to reference ESICR to existing datasets but we will let the users of our dataset judge whether it is better than others. The motivation for this dataset is clearly described in the introduction, in particular points 1-4 describing a new methodology for processing sea ice concentration which is at the same time an answer to some problematic issues in the processing of previous datasets (1. sensitivity to atmospheric and surface emissivity trends: "artificial trends", 2. no noise reduction over both ice and water, 3. inter-sensor calibration issues, 4. no uncertainties). The fourth point: we have for the first time provided a dataset with spatially and temporally varying uncertainties along with the sea ice concentration. I think this is a convincing improvement compared to existing datasets and sufficient motivation for the reprocessing. In addition, as we mention in "future work" the dataset and the methodology for processing it are still being developed and this will be implemented in future updates.

Anyway, your comment is valid in order to relate ESICR to other datasets and we have therefore included a comparison between ESICR and the NSIDC sea ice extent and a discussion of the differences (new section 3.4 and an extra column in Tab. 3A and 3B).

2. A routine Similarity Assessment has revealed that your manuscript has a similarity index of 24% compared to previously published work. This is unusually high compared with other manuscripts. A closer

inspection revealed that approximately 20% of your manuscript was more or less copied literally from initial OSISAF reports (Tonboe and Nielsen, 2011; and Eastwood et al., 2010). As this is your own work, I think you cannot be accused of fraud; however, it would be important to cite those reports and to put your work into context and to point out the basis (and substantial historical experience) that has gone into it.

Reply:

Thanks, these two references appear together with the dataset at osisaf.met.no and of course these should also be included in the text and reference list of this MS. They are now included in the introduction explaining what they are and where to find them.

The EUMETSAT sea ice concentration climate data record

~~R.~~Rasmus¹, T. Tonboe¹, ~~S.~~Steinar Eastwood², ~~F.~~Thomas Lavergne², ~~A.~~Atle M. Sørensen², ~~N.~~Nicholas Rathmann³, ~~G.~~Gorm Dybkjær¹, ~~L.~~Leif Toudal Pedersen¹, ~~J.~~Jacob L. Hoyer¹, ~~S.~~Stefan Kern⁴

¹Danish Meteorological Institute, Lyngbyvej 100, Copenhagen, DK-2100, Denmark

²Norwegian Meteorological Institute, P.O.BOX 43, Oslo, N-0313, Norway

³University of Copenhagen, Juliane Maries Vej 30, Copenhagen, DK-2100, Denmark

⁴University⁴Integrated Climate Data Center (ICDC) University of Hamburg, Grindelberg 5, Hamburg, D-20144, Germany

Correspondence to: R. T. Tonboe (rtt@dmi.dk)

Abstract. An Arctic and Antarctic sea ice area and extent dataset has been generated by EUMETSAT's Ocean and Sea Ice Satellite Application Facility (OSISAF) using the record of microwave radiometer data from NASA's Nimbus 7 Scanning Multichannel Microwave radiometer (SMMR) and the Defense Meteorological satellite Program (DMSP) Special Sensor Microwave/Imager (SSM/I) and Special Sensor Microwave Imager and Sounder (SSMIS) satellite sensors. The dataset covers the period from Oct. 1978 to Apr. 2015 and updates and further developments are planned for the next phase of the project. The methodology for computing the sea ice concentration is using: 1) numerical weather prediction (NWP) data input to a radiative transfer model (RTM) for ~~correction~~reduction of the ~~brightness temperatures for reducing the~~ impact of weather conditions on the measured brightness temperatures (~~T_b~~), 2) dynamical algorithm tie-points to mitigate trends in residual atmospheric, sea ice and water emission characteristics and inter-sensor differences/biases, ~~3)~~ and 3) a hybrid sea ice concentration algorithm using the Bristol algorithm over ice and the Bootstrap algorithm in frequency mode over open water. A new sea ice concentration uncertainty algorithm has been developed to estimate the spatial and temporal ~~variabilities~~variability in sea ice concentration retrieval accuracy. A comparison to U.S. National Ice Center sea ice charts from the Arctic and the Antarctic shows that ice concentrations are higher in the ice charts than estimated from the radiometer data at intermediate sea ice concentrations in between open water and 100% ice. The sea ice concentration climate ~~dataset~~data record is available for download at (www.osisafosi-saf.org), including documentation.

1. Introduction

The Arctic sea ice covered area and extent has decreased since the 1970s (Cavalieri and Parkinson, 2012). In Antarctica there are large regional differences in trends but overall the sea ice extent is increasing because of changing atmospheric circulation patterns and regional cooling (Comiso et al., 2011); ~~Holland and Kwok, 2012~~. The climatic trends in sea ice extent have been documented using models (Zhang and Walsh, 2006; ~~Goosse and Zunz, 2014~~), ice charts (Rayner et al., 2003) and in particular the passive microwave data record from U.S. satellite microwave radiometers (Parkinson and Cavalieri, 2012; Cavalieri and Parkinson, 2012). Throughout this paper the sea ice extent is defined as ice covered waters with ice concentrations derived from microwave radiometer data greater than 30% and at a grid resolution of 12.5 x 12.5 kilometerskm.

The brightness temperatures measured by the satellite radiometers at the atmospheric window channels are dominated by surface emission. However, the measured brightness temperatures are also affected by weather conditions such as wind roughening of the ocean surface, water vapor and cloud liquid water (Wentz, 1983 and 1997; Andersen et al., 2006B). These parameters have trends over the observing period (Wentz et al., 2007). Even though the sensitivity to these parameters is minimized in ice concentration algorithms in general, different algorithms still have different sensitivities (Andersen et al., 2006B). Here we define the noise as the ice concentration fluctuations caused by the instrument electronic components, ice and water surface emissivity variability and weather conditions, i.e. estimated ice concentration variability not caused by changes in the actual ice concentration.

Because of the ~~algorithms~~algorithms' different sensitivities to the noise, and that the noise has climatic

Formateret: Linjeafstand: enkelt

Formateret: Engelsk (Storbritannien)

Formateret: Engelsk (Storbritannien)

Formateret: Engelsk (Storbritannien)

Formateret: Engelsk (Storbritannien)

Formateret: Engelsk (Storbritannien)

Formateret: Engelsk (Storbritannien)

Formateret: Engelsk (Storbritannien)

Formateret: Engelsk (Storbritannien)

Formateret: Engelsk (Storbritannien)

Formateret: Linjeafstand: enkelt

Formateret: Indrykning: Hængende: 0,63 cm, Linjeafstand: enkelt

Formateret: Linjeafstand: enkelt

1 | trends, the differences- also appear as trends in the sea ice extent trends (Andersen et al., 2007). To
2 | minimize these artificial trends caused by noise we must: 1) find algorithms with low sensitivities to
3 | the atmospheric and surface emissivity variability, 2) correct the brightness temperatures for the
4 | properties that we are able to quantify (numerical weather prediction (NWP) data: near surface wind;
5 | and air temperature and columnar atmospheric water vapor content), and in particular when doing this
6 | it is important to 3) calibrate the algorithms to the actual ice and water signatures using dynamical tie-
7 | points, and finally 4) quantify the residual uncertainties. The EUMETSAT sea ice concentration
8 | climate data record (ESICR) is generated according to these principles, 1 - 4, and it is based on the
9 | NASA's Nimbus 7 Scanning Multichannel Microwave Radiometer (SMMR) (1978-1987), the DMSP's
10 | Special Sensor Microwave/Imager (SSM/I) (1987-2009) and the DMSP's Special Sensor Microwave
11 | Imager and Sounder (SSMIS) (2003-today) radiometer data. It uses a combination of the Bristol
12 | (Smith, 1996) and the Bootstrap (Comiso, 1986) algorithms with dynamical tie-points, explicit
13 | atmospheric correction using NWP data for error reduction and it comes with spatially and temporally
14 | varying sea ice concentration uncertainty estimates describing the sea ice concentration accuracy.
15 | Dynamical tie-points are typical signatures of sea ice and water used in required to compute the sea-ice
16 | concentration algorithms to scale from the ice concentration measured brightness temperatures. These
17 | are derived on a daily basis for each hemisphere and therefore adjust the algorithms to the current
18 | signatures of ice and water (see section 2.1).

19 |
20 | The sea ice concentration uncertainty estimates are needed when the ice concentration data are
21 | compared to other data sets or when the ice concentrations are assimilated into numerical models. The
22 | mean accuracy of some of the more common algorithms, used to compute ice concentration from
23 | SSM/I data, such as the NASA Team and Bootstrap are reported to be 1-6% in winter (Steffen and
24 | Schweiger, 1991; Emery et al., 1994; Belchansky and Douglas, 2002). The overall accuracy of the
25 | SMMR total ice concentrations is estimated to be $\pm 7\%$ (Gloersen et al., 1992). During summer the
26 | uncertainties are larger than during winter (Ivanova et al., 2015).

27 |
28 | The ESICR data are available at the EUMETSAT OSISAF homepage (osisaf.met.no) including the
29 | validation report (Tonboe et al., 2015) and the product user manual (Eastwood et al., 2015).

30 | 31 | 32 | **1.1 Description of the Nimbus 7 SMMR instrument and data**

33 | The SMMR instrument on board the Nimbus 7 satellite operated from ~~Oct. October~~ 1978 to
34 | ~~Aug. August~~ 1987 (Gloersen et al., 1992). The instrument had 10 channels at five frequencies (6.6,
35 | 10.7, 18.0, 21.0, 37.0 GHz) and vertical (v) and horizontal (h) linear polarization. Each of the channels
36 | has different spatial resolution on the ground spanning from 148 x 95 km at 6 GHz to 27 x 18 km at 37
37 | GHz. The across track scanning was accomplished by tilting the reflector from side to side while
38 | maintaining a constant incidence angle on the ground of about 50.2°. The scan track on the ground
39 | formed a 780 km wide arc in front of the satellite (Gloersen and Barath, 1977). Because of the satellite
40 | orbit inclination and swath width there is no coverage pole-wards of 84°. SMMR data were acquired
41 | every second day because of satellite power limitations. Data were provided by the National Snow and
42 | Ice Data Center (NSIDC) as brightness temperatures in swath projection (Meier, 2008).

43 | 44 | **1.2 Description of the SSM/I and SSMIS instruments and data.**

45 | The SSM/I instruments onboard the DMSP satellites are conically scanning instruments with seven
46 | total power radiometers measuring channels at 19.35v, 19.35h, 22.2h, 37.0v, 37.0h, 85.5v, and 85.5h.
47 | The spatial resolution on the ground is 69 x 43 km at 19 GHz and 15 x 13 km at 85 GHz. The incidence
48 | angle is 53.1° and the swath width on the Earth's surface is about 1400 km. There is no coverage pole-
49 | wards of 87°-° for the same reason as for SMMR (section 1.1). The different satellites and their
50 | operation periods are listed in Table 2. The SSM/I data (version 6 and not the newer version 7) was
51 | purchased by EUMETSAT from Remote Sensing Systems (RSS) as antenna temperatures and
52 | converted to brightness temperatures using RSS software. The RSS SSM/I version 6 post processing
53 | includes geo-location correction, sensor calibration and quality control procedures, and inter calibration
54 | between the different satellites from overlapping periods. These procedures are documented in the RSS
55 | SSM/I User's Manuals (Wentz, 1991; Wentz, 1993; Wentz, 2006).

56 |
57 | The SSMIS is a continuation of the SSM/I series of instruments onboard the DMSP satellites but with
58 | an extension in the number of channels. SSMIS has 24 channels between 19 and 183 GHz. The 19 and
59 | 37 GHz channels which are used in the ESICR have identical frequencies on SSM/I and SSMIS.
60 | However, SSMIS has a swath width of about 1700km which gives near complete daily coverage of the

Formateret: Linjefast: enkelt

1 Arctic Ocean. The SSMIS data are from the L2B near real time data-stream issued via EUMETCast
2 and processed at the U.S. National Ocean and Atmospheric Administration (NOAA).

3 4 **1.3 Meteorological data**

5 The NWP model meteorological data are used for reduction of the brightness temperatures for
6 atmospheric noise with a radiative transfer model. European Centre for Medium-range Weather
7 Forecast (ECMWF) ERA 40 data are used for the period from 1978 to 2002, and ECMWF data from
8 the operational models are used from 2002 onwards. A description of the ERA 40 meteorological data
9 archive and the reanalysis can be found in Kålberg et al. (2004). ~~The ERA data are at 6 hourly temporal
10 and 1.25° spatial resolution.~~

11 12 **1.4 MODIS data**

13 The coarse resolution of the passive microwave brightness temperature measurements gives rise to an
14 additional uncertainty when sea ice concentration is ~~reproduced~~ computed at finer grid spacing. We call
15 this the smearing uncertainty and it is estimated using a smearing model (see section 2.54.2). High
16 resolution ice concentration data are used as input to the smearing model: Cloud free and non-
17 calibrated MODIS Moderate Resolution Imaging Spectroradiometer (MODIS) scenes from the NASA
18 image gallery archive (<http://rapidfire.sci.gsfc.nasa.gov/cgi-bin/imagery/gallery.cgi>) were selected
19 manually for their different sea ice conditions: low concentration, medium and high concentration.
20 Parts of the image with cloud cover were cut out manually. The band 1 (620 - 670 nm) brightness
21 (given as pixel values between 0 and 255) is high - typically greater than 220 for sea ice and less than
22 60 for open water. These two upper and lower values are used for scaling pixels between 100% and 0%
23 ice concentration respectively. Pixels with intermediate brightness are assigned intermediate
24 concentrations linearly. Brightness pixels with a brightness above 220 and below 60 ~~is truncated to are~~
25 assigned sea-ice concentrations of 100% and 0% respectively. The 250 m spatial resolution is re-
26 sampled to 1 km pixel resolution.

27 28 **1.5 Ice chart data for comparison**

29 The operational sea ice charts from the U.S. National Ice Center (NIC) are used for comparison with
30 the ESICR sea ice concentration. The ice charts, intended for aiding navigation, are produced on a
31 weekly basis covering all seasons, both ~~Southern~~ southern and ~~Northern~~ northern hemispheres and the
32 time series cover the entire climate record period except for the period Dec. 1994 to Jan. 2006 on the
33 ~~Southern~~ southern hemisphere. The ice charts used for comparison are a combination of three datasets:
34 1) The NIC ice charts for the ~~Northern Hemisphere~~ northern hemisphere 1972-2007 available at
35 National Snow and Ice Data Center (NSIDC) in gridded format (Fetterer and Fowler, 2009), 2) the NIC
36 ice charts for the southern hemisphere 1973-1994 available at (~~Fetterer, the NSIDC (Fetterer,~~ 2006),
37 and 3) the NIC ice charts for both hemispheres from 2006-2015 available from NIC.

38
39 The more recent ice charts are based partly on satellite Synthetic Aperture Radar (SAR) data e.g.
40 RADARSAT 1 since 1995 and ENVISAT since 2002, various scatterometers together with
41 visual/infrared line scanners e.g. Advanced Very High Resolution Radiometer (AVHRR), MODIS,
42 Operational Linescan System (OLS) whenever possible for daylight and cloud cover conditions. Also
43 the passive microwave data from SMMR and ~~SMM~~ SSM/I used in this re-processing of ice
44 concentrations have been extensively used for making the ice charts in particular before the launch of
45 wide swath SAR instruments in 1995. In addition to the satellite data, ice charts are based on
46 information from ships and aircraft reconnaissance. ~~The~~ For an ice chart different sea ice categories are
47 delineated manually by polygons and assigned a range of sea ice concentrations, thicknesses, type etc.
48 found within the polygon ~~in the ice chart~~ by an ice analyst. This information is represented on the
49 satellite pixel grid by averaging the range of ice concentrations and other properties given within the
50 polygon (Dedrick et al., 2001).

51 52 **2.0 Methodology**

53 **2.1 Dynamical tie-points**

54 Tie-points are typical signatures of ice and open water which are used in the ice concentration
55 algorithms as a reference. The tie-points are derived by selecting brightness temperatures from regions
56 of known open water and ice.

57
58 During winter, in the consolidated pack ice well away from the ice edge, the ice concentration is very
59 near 100 %. This has been established using high resolution SAR data, ship observations and by
60 comparing the estimates from different ice concentration algorithms (Andersen et al., 2007). The

1 apparent fluctuations in the derived ice concentration in the near 100 % ice regime are primarily
 2 attributed to variations in snow/ice surface emissivity and temperature-~~and atmospheric variability~~
 3 around the tie-point signature and only secondarily to actual ice concentration fluctuations. In the
 4 marginal ice zone at intermediate ice concentrations and over open water the atmospheric emission and
 5 wind-~~shear-induced water surface roughness~~ and smearing dominates as error sources. ~~There is no~~
 6 ~~explicit correction for cloud liquid water and this is an uncertainty source over both ice and open water.~~
 7 The ice concentration algorithm sensitivity -to atmospheric and surface emission are systematic,
 8 meaning that different algorithms with different sensitivity to atmospheric and surface emission
 9 ~~compute can provide~~ very different trends in sea ice extent on seasonal and decadal time scales
 10 (Andersen et al., 2007). This means that not only does the estimated sea ice extent have a climatic
 11 trend; also the atmospheric and surface constituents affecting the microwave emission are changing. In
 12 an attempt to compensate for the influence of these artificial trends, the tie-points are derived
 13 dynamically using a window of width ± 15 days centered at the day of the actual sea ice concentration
 14 retrieval. It is assumed that ice concentrations greater than 95 % from the NASA Team algorithm
 15 (Cavalieri et al., 1984) are in fact a representation of near 100 % ice. The NASA Team algorithm has
 16 different sensitivities to artificial trends than the two algorithms used in combination here (Andersen et
 17 al., 2007). The ice tie-point is the mean brightness temperature value of ~~these selected~~ all data points
 18 with greater than 95 % NASA-Team sea-ice concentration within the ± 15 days window. The static
 19 NASA Team tie-points for SMMR are found in Gloersen et al. (1992) and for SSM/I the tie-points are
 20 found in Andersen (1998). Geographically, the sea ice tie-point is excluding data of both the SMMR
 21 and the SSM/I instruments pole-wards of 84° for consistency between the SMMR and SSM/I periods.
 22 The open water tie-point data were selected geographically along two belts on the northern and
 23 southern hemisphere respectively (between 53°N and 75°N and between 65°S and 80°S). A land mask
 24 including the coastal zone and sea ice maximum extent climatology ensures open water data only.

25
 26 There is no attempt to compensate explicitly for sensor drift or inter-sensor calibration differences
 27 (even though the SSM/I data have been inter-calibrated by RSS) or possible biases in the NWP fields
 28 used for atmospheric noise reduction of the brightness temperatures. The dynamical tie-point method is
 29 in principle compensating for these problems in a consistent manner.

30
 31 **2.2 Atmospheric noise reduction of the brightness temperatures using NWP data**

32 Using an emission model, the brightness temperatures are corrected for the influence of water vapor in
 33 the atmosphere and open water surface roughness caused by wind. The emission model used for
 34 atmospheric noise reduction of the SMMR brightness temperatures, T_b , with NWP input is (Wentz,
 35 1983):

36
$$T_b = f(T_s, u^*, V, L, T_a) \quad (1),$$

37 where T_s is the physical surface temperature, u^* is the sea surface wind friction velocity, V is the
 38 integrated atmospheric water vapor column, L is the atmospheric liquid water column, and T_a is the
 39 surface (at 2 m) air temperature. A similar model is used for the SSM/I and SSMIS data (Wentz, 1997).

40 Over areas with both ice and water the influence of open water roughness on the brightness
 41 temperatures and the ice emissivity is scaled linearly with the ice concentration. The emissivity of ice is
 42 given by standard tie-point ~~emissivities~~ emissivity values and the total ice concentration is solved by
 43 iteration with a first guess of the ice concentration from the NASA Team algorithm (Cavalieri et al.,
 44 1984) with static tie-points. The correction procedure is described in detail in Andersen et al. (2006B).
 45 The NWP model grid points are co-located with the satellite swath data in time (maximum three hours)
 46 and space using linear interpolation and a correction to the brightness temperatures using Eq. 1 is
 47 applied. The potential inconsistencies between the ERA40 and the operational ECWMF models are
 48 minimized by the dynamical tie-point adjustment later in the processing and eventually the residual
 49 error is included in the error estimate.

50
 51 The representation of atmospheric liquid water column in the NWP data is not suitable to use for
 52 brightness temperature correction because of the spatial and temporal variability of clouds which is
 53 higher than the model grid cell size and model time step size. The ~~data~~ brightness temperatures are
 54 therefore not corrected for the influence of atmospheric liquid water. Assuming a neutral atmospheric
 55 temperature profile, the wind speed at 10 m, given by the numerical weather prediction model, is
 56 converted to the surface friction velocity using the factor 0.047 for use in the SMMR RTM. The other
 57 NWP variables are used directly.

58
 59
 60 **2.3 The ice concentration algorithm**

Formateret: Skriftype: Kursiv
 Formateret: Skriftype: Kursiv
 Formateret: Skriftype: Kursiv
 Formateret: Skriftype: Kursiv
 Formateret: Skriftype: Kursiv

1 | The analysis of atmospheric sensitivity in Andersen et al. (2006B) showed that the Bootstrap frequency
2 | mode algorithm (Comiso, 1986; Comiso et al., 1997) had the lowest sensitivity to atmospheric noise at
3 | low ice concentrations. Furthermore, the comparison to high resolution SAR imagery in Andersen et al.
4 | (2007) indicated that among the algorithms using 19 and 37 GHz channels available on both SMMR
5 | and SSM/I - SSMIS, the Bristol algorithm (Smith, 1996) had the lowest sensitivity to ice surface
6 | emissivity variability. In addition the Bristol algorithm had low sensitivity to atmospheric emission in
7 | particular at high ice concentrations.

8 |
9 | Consequently, we use a combination of the Bristol algorithm and the Bootstrap frequency mode
10 | algorithm. ~~_____ a so-called hybrid algorithm.~~

11 | ~~The original Bootstrap sea ice concentration algorithm is a combination of two algorithms: the~~
12 | ~~polarization mode algorithm which is used over ice and the frequency mode algorithm which is used~~
13 | ~~over open water (Comiso, 1986). Only the Bootstrap algorithm in frequency mode, the open water part,~~
14 | ~~is used here. The Bootstrap frequency mode algorithm uses T_{19v} and T_{37v} .~~ The algorithm assumes only
15 | two surface types: ice and open water. The linear relationship yields the following formulation for the
16 | total sea ice concentration, ic :

$$17 | ic_{Bootstrap} = (Tb - \cancel{Tb^W}) / (Tb^I - Tb^W) / (Tb^I + Tb^W), \quad (2)$$

18 | where Tb is the measured brightness temperature, Tb^W is the open water tie-point, and Tb^I is the ice tie-
19 | point.

20 |
21 | The Bristol algorithm (Smith, 1996) is conceptually similar to the Bootstrap algorithm. In a three-
22 | dimensional scatter plot spanned by T_{19v} , T_{37v} and T_{37h} the ice points tend to fit a plane surface. The
23 | only difference to the Bootstrap algorithm is that instead of viewing the data in the T_{19v} , T_{37v} space, the
24 | Bristol algorithm views the data perpendicular to the data plane, ~~i.e. that contains both the ice line and~~
25 | ~~the water tie-point i.e.~~ in a transformed coordinate system:

$$26 | 1. \text{ axis: } T_{37v} + 1.045T_{37h} + 0.525T_{19v}, \quad (3a)$$

$$27 | 2. \text{ axis: } 0.9164T_{19v} - T_{37v} + 0.4965T_{37h}. \quad (3b)$$

28 | The remaining analysis is identical to the Bootstrap algorithm.

29 | The Bootstrap algorithm is used over open water and the Bristol algorithm is used over ice. At
30 | intermediate concentrations up to 40% (from the Bootstrap ice concentration estimate) the ice
31 | concentration is an average weighted linearly between the two algorithms i.e.

$$32 | ic = (1 - wc) * ic_{Bristol} + wc * ic_{Bootstrap} \quad (4a),$$

33 | where

$$34 | wc = (|t - ic_{Bootstrap}| + t - ic_{Bootstrap}) / (2 * t) \quad (4b),$$

35 | where t is the threshold of 40%.

37 | 2.54 The sea ice concentration uncertainties

38 | The uncertainties described in the following sections are generally independent and the squared sum of
39 | the two estimated components of uncertainty is assumed to represent the total uncertainty squared.

40 | Each of the components is quantified as the standard deviation of sea ice concentration. The tie-point
41 | uncertainty $\epsilon_{tie-point}$, including residual atmospheric noise, sensor noise and ice surface emissivity
42 | variability, is derived from measurements as the first component of uncertainty. The representativeness
43 | error, ϵ_{smear} , is simulated using a model as the second component of uncertainty, i.e.

$$44 | \epsilon_{total}^2 = \epsilon_{tie-point}^2 + \epsilon_{smear}^2 \quad (5).$$

45 |
46 | In addition to these two sea ice concentration uncertainty components there is the geo-location error. It
47 | occurs when the satellite is not exactly oriented (Poe et al., 2008). Simulations show that because of the
48 | large footprints (see next section for footprint sizes) compared to the typical geo-location errors of the
49 | SSM/I (about ± 5 km, Hollinger et al., 1990) the ice concentration uncertainty due to geo-location errors
50 | is small and neglected here. ~~Locally~~ There may be regions along the ice edge and along coastlines

Formateret: Linjefast: enkelt,
Tabulatorstop: Ikke med 2,36 cm

Formateret: Linjefast: enkelt

Formateret: Skrifttype: Kursiv

Formateret: Skrifttype: Kursiv

Formateret: Skrifttype: Kursiv

Formateret: Skrifttype: Kursiv

Formateret: Linjefast: enkelt

1 | where the geo-location errors may be significant ~~but difficult~~. However, we have not been able to
2 | include these errors in the sea ice concentration uncertainty estimate.

3 | **2.5.4.1 First component: instrument noise, algorithm and tie-point uncertainties**

4 | Both the water surface and ice surface emissivity variability and emission and scattering in the
5 | atmosphere affects the brightness temperatures and the computed ice concentrations. ~~Different~~
6 | ~~algorithms have different sensitivities to these surface and atmospheric parameters (Andersen et al.,~~
7 | ~~2006B). Further, both the atmospheric and surface parameters affecting the ice concentration estimates~~
8 | ~~have climatic trends (Andersen et al., 2007).~~ To reduce the uncertainties due to atmospheric noise, the
9 | brightness temperatures are corrected using NWP data for atmospheric water vapor, near surface air
10 | temperature and open water roughness caused by wind. The remaining tie-point uncertainties are given
11 | as the tie point ice concentration standard deviation in regions with open water or 100% ice.

12 |
13 | Random instrument noise also results in ice concentration uncertainties. The SSM/I instrument noise
14 | results in an ice concentration uncertainty of 1.4 % for the Bristol algorithm, and 1.7 % for the
15 | Bootstrap algorithm in frequency mode (Andersen et al., 2006A). Systematic sensor drift is critical
16 | issue for ice concentration algorithms using static tie-points. Here we use dynamical tie-points intended
17 | for alleviating problems with sensor drift, and inter-sensor calibration.

18 | **2.5.4.2 Second component: the representativeness error**

19 |
20 |
21 | Footprint sizes for the channels used for ice concentration mapping are uneven and range from about
22 | 50-70 km for the 19 GHz channels to about 30 km for the 37 GHz channels. ~~Footprints of uneven size~~
23 | ~~are combined in the algorithms when computing the ice concentration. The footprint ice concentration~~
24 | ~~is represented on a predefined sampling grid.~~ The ice concentration data are normally represented on a
25 | finer grid (typically 12.5 or 25 km) than the sensor ~~resolution~~ footprint sizes (30 to 70 km). This effect
26 | is called smearing. The combination of footprints of uneven size in the ice concentration algorithm
27 | results in an additional smearing effect. This we call the footprint mismatch error. The smearing and
28 | the footprint mismatch error cannot be estimated separately. However, the combined error can be
29 | estimated if all other error sources and the ice cover reference are known a priori. It can also be
30 | simulated using high resolution ice concentration reference data and a model for the satellite
31 | measurement footprint patterns. Here we use the model ~~described in section 2.5.3~~.

32 | **2.5.3 Simulating the smearing uncertainty**

33 |
34 | The smearing simulation model uses high resolution brightness temperature input to compute the
35 | brightness temperatures as would be measured by the coarse resolution radiometers on board the
36 | satellite. The high resolution input is compared to the coarse resolution output and realizations of ice
37 | concentrations in the hybrid sea ice concentration algorithm.

38 |
39 | Reference SIC is derived from the brightness of cloud-free MODIS scenes re-sampled to 1-~~km~~ x 1 km
40 | pixel size described in section 1.4. The MODIS pixel brightness across the image may vary slightly as
41 | a function of solar angle and albedo (snow type, and sea ice type) leading to uncertainties in the derived
42 | ice concentration. However, here it is the reference and it does in fact provide a realistic spatial
43 | distribution of ice at the right scale for input to the model and as a reference for comparison. Each of
44 | these 1-~~km~~ x 1 km ice concentration pixels is assigned a microwave brightness temperature using
45 | standard tie-points (Comiso et al., 1997) and linear mixing between 0 and 100%. For each 1-~~km~~ x 1
46 | km brightness temperature pixel elliptical Gauss-shaped antenna patterns (Drusch et al., 1999) are used
47 | to simulate brightness temperatures at 19v and 19h, 37v and 37h as it would be measured with SMMR
48 | and SSM/I ~~or~~ SSMIS on the satellite. The simulations of brightness temperatures are used as input to
49 | the Comiso Bootstrap frequency mode (CF) and Bristol algorithms using standard tie-points. The
50 | resulting ice concentration estimate is then compared to the ice concentration reference from MODIS
51 | sampled to different resolutions, i.e. 1, 5, 10, 12, 25 and 50 km (see table Tab. 2). The STD between the
52 | truth at a certain pixel resolution and the simulated satellite image is the smearing uncertainty. The
53 | smearing uncertainty is assumed uniform between $0\% + \epsilon_{\text{tiepoint}}$ and $100\% - \epsilon_{\text{tiepoint}}$. At 0% and at 100
54 | % it is zero. Table 2 shows the smearing uncertainty for the CF, the Bristol and the average hybrid
55 | OSISAF algorithm STD ~~of the difference~~ at different grid resolutions. The final grid resolution of the
56 | ESICR obtained with the OSISAF algorithm is 12 km ~~which means that the and has a~~ smearing
57 | uncertainty ~~is of~~ 12% (Tab. 2). The smearing uncertainty is nearly the same for the CF and the
58 | Bristol algorithms.

Formateret: Linjefastand: enkelt

Formateret: Linjefastand: enkelt

1 The MODIS image used for estimating the smearing uncertainty is shown in Figure 1. The image has
2 regions of open water, intermediate concentrations and of ~~complete 100 %~~ ice cover. The simulated
3 SSM/I sea ice concentration using Figure 1 as input to the ~~OSISAF~~ ~~Hybrid OSISAF~~ algorithm is shown
4 in Figure 2.

6 **2.5.4.3 The sea ice concentration uncertainty algorithm**

7 The representativeness uncertainty is computed as a function of ice concentration using a model. The
8 other error sources are computed using the hemispheric standard deviation of the ~~measurements~~ ~~ice~~
9 ~~concentration estimates~~ over open water and over near 100 % ice respectively. The ice concentration
10 algorithm provides ice concentrations which are greater than 100% ~~and less than 0% - % and less than 0~~
11 ~~% because of the natural variability of the measured brightness temperatures around the ice and open~~
12 ~~water tie points~~. These unphysical concentrations are truncated in the processing. ic is the ice
13 concentration calculated by the algorithm and α is the truncated ice concentration (constrained to the
14 interval 0 - 100 %):

15 if $ic \leq 0$ then $\alpha = 0$

16 if $0 < ic < 1$ then $\alpha = ic$ (6)

17 if $ic \geq 1$ then $\alpha = 1$

18
19 Using ~~equation~~ Eq. 2 and assuming the uncertainty for the ice and water part is independent this leads to
20 a total tie-point uncertainty ~~ieof~~

$$21 \varepsilon_{tie-point}(\alpha(ic)) = \sqrt{(1 - \alpha(ic))^2 \varepsilon_{water}^2 + \alpha^2(ic) \varepsilon_{ice}^2} \quad (7)$$

$$22 \text{ where } \varepsilon_{water} = \varepsilon(IC(P_{water})) \quad (8),$$

23
24 and open water is determined from open water measurements near the ice edge. IC is the functional
25 mapping of the ice concentration algorithm and P_{water} denotes the set of ~~open water~~ swath pixels for all
26 swaths (used for calculating the daily product).

$$27 \varepsilon_{ice} = \varepsilon(IC(P_{NT > 0.95})) \quad (9),$$

28
29 is the STD of the ice concentrations where ~~the NASA team (NT) algorithm estimates Team~~ ice
30 concentrations ~~are~~ greater than ~~0.95 %~~.

31 The ice concentration uncertainty is a function of sea ice concentration (Fig. 3) where the total

32 uncertainty squared is the sum of the two uncertainty components squared (see ~~eq. 4~~ Eq. 5). The

33 smearing uncertainty is zero for open water and for 100 % ice and at these two points on the curve the

34 total uncertainty ~~is equals~~ the tie-point uncertainty (including sensor and residual atmospheric noise)

35 for open water and ice respectively: (see Eqs. 6 and 7). The smearing uncertainty reaches a maximum

36 at intermediate concentrations between $(0\% + \varepsilon_{tiepoint})$ and $(100\% - \varepsilon_{tiepoint})$. ~~Uncertainty for ice~~

37 ~~concentrations smaller than 0% and greater than 100% is the tie-point uncertainty.~~

38 Because the sea ice concentration is provided on a relatively fine grid of about 12.5 km compared to
39 the actual resolution of the sensor the smearing uncertainty is the component which is dominating the
40 total uncertainty: ~~for most of the sea-ice concentration range (Fig. 3)~~. When the grid resolution is
41 comparable to the ~~actual spatial resolution footprint size~~ of the ~~algorithm at sensor, i.e. in our case about~~
42 50 km, the smearing uncertainty (see ~~Table~~ Tab. 2) ~~become~~ ~~becomes~~ comparable in magnitude to the
43 tie-point uncertainty which is where the total uncertainty is at a minimum.

44 **2.6 From level 2 swath projection data to interpolated level 4 maps**

45 The transition from level 2 swath projection data to the final level 4 daily predefined EASE grid
46 includes the gridding of the swath data, the filtering of coast line grid cells, the maximum ice extent
47

Formateret: Skrifttype: Kursiv

Formateret: Skrifttype: Kursiv

Formateret: Skrifttype: Kursiv

Formateret: Skrifttype: Kursiv

Formateret: Skrifttype: Kursiv

Formateret: Skrifttype: Kursiv

Formateret: Skrifttype: Kursiv

Formateret: Skrifttype: Kursiv

Formateret: Skrifttype: Kursiv

Formateret: Skrifttype: Kursiv

Formateret: Skrifttype: Kursiv

Formateret: Skrifttype: Kursiv

Formateret: Skrifttype: Kursiv

Formateret: Linjeafstand: enkelt

1 masking and spatial and temporal interpolation- of data gaps. Whenever a pixel is altered by any of
2 these processing steps it is ~~at the same time~~ indicated with a flag value in the product file.

3
4 The time window of 24 hours is centered at 12:00 UTC. The ice concentration swath data is averaged
5 for each grid cell using the simple weighting function:

$$6 \quad weight = 1 - 0.3 * (dist/inflrad) \quad (10),$$

7
8 where *dist* is the distance between the data point center and the grid cell center and *inflrad* is the radius
9 of influence (18 km). All data from overlapping missions are included in the gridding except the
10 overlap between SMMR and SSM/I. Only the SSM/I data are used during the overlap of 1.5 months
11 between SMMR and SSM/I.
12

13 **2.65.1 Statistical filtering of ice concentration near the coastline**

14
15
16 Due to the coarse spatial resolution of the radiometers the data may be influenced by land up to 70 km
17 from the coastline. The emissivity of land along the coastline is comparable to sea ice emissivity and
18 much higher than water emissivity. This means that in the coastal zone, if there is open water or
19 intermediate concentrations, the sea ice concentration will be overestimated. The statistical method
20 which is described in Cavalieri et al. (1999) is used for filtering the ice concentration near the coast.

Formateret: Linjeafstand: enkelt

Formateret: Skrifttype: Ikke Fed

21 22 23 **2.65.2 Climatological maximum sea ice extent masking**

24 Occasionally spurious sea ice is detected in open water regions far from the ice edge due to
25 atmospheric noise affecting the ice concentration estimate. These spurious sea ice detections are
26 masked out using the monthly maximum extent climatology by the NSIDC
27 (http://nsidc.org/data/smmr_ssmi_ancillary/ocean_masks.html). ~~A zone of additional 100 km into the~~
28 ~~open water has been added to~~ Within a month the position of the daily sea-ice edge can fluctuate
29 substantially and it might cross the border of the maximum extent climatology used. Therefore, in order
30 to not generally limit the ice extent to ~~ensure~~ this climatology and allow detection of real sea ice also
31 outside of the climatology, ~~we added a zone of additional 100 km into the open water.~~
32

Formateret: Linjeafstand: enkelt

33 **2.65.3 Level 4: Gap filling by spatial and temporal interpolation**

34 Grid cells with missing data are filled with interpolated values in the level 4 processing and the affected
35 pixels are flagged. Daily data coverage is never complete due to the ~~hole~~ observation gap near the North
36 Pole (see sections 1.1 and 1.2) and occasionally there are missing scan lines, and missing orbits. Spatial
37 interpolation can fill small gaps e.g. one or two missing scan lines but it is deceiving when large areas
38 are missing and filled with interpolated values. To overcome this issue, yet implementing a general
39 approach for all cases, both temporal and spatial interpolation is used.

40 The weighting parameters are computed as follows:

$$41 \quad w_{i,j}^D = 1/(\sigma_{i,j}^D)^2 (2N_{max} + 1) \quad (11)$$

$$42 \quad W^D(k, l; i, j) = 1/(\sigma_{k,l}^D)^2 \times \exp(-0.5(\frac{\Delta(k,l;i,j)}{R_{i,j}})^2) \quad (12),$$

43 where σ is the standard deviation associated to each ice concentration estimate, Δ is the distance
44 between a given (k,l) neighbor and cell (i,j) and R is an auto-correlation radius. The spatial
45 interpolation weight is thus based on an isotropic Gaussian distribution, and almost all (>99.9%) of the
46 interpolation weight is concentrated inside a $[-3R;+3R] \times [-3R;+3R]$ km² area, which translates into a $[-$
47 $N_{max};+N_{max}] \times [-N_{max};+N_{max}]$ grid cells squared area. It was found by testing that R is proportional to the
48 absolute latitude in degrees, i.e. $R = \text{latitude of } (i,j)$.

49 The interpolation on a given date, D , uses data from the day before and the day after, i.e. $D-1$, ~~D~~ and
50 $D+1$.

51 The interpolated value at grid cell (i,j) for day D is given by:

$$52 \quad X_{i,j}^D = K(w_{i,j}^{D-1}X_{i,j}^{D-1} + w_{i,j}^{D+1}X_{i,j}^{D+1} + \sum_{k,l} W^D(k, l; i, j)X_{k,l}^D) \quad (13),$$

53 where X is the sea ice concentration value and K is a normalizing factor given by:
54

$$w_{i,j}^{D-1} + w_{i,j}^{D+1} + \sum_{k,l} W^D(k, l; i, j) = 1/k \quad (14).$$

The spatial interpolation from neighbors of cell (i,j) in [equation Eq. 13](#) is only using values from date D , while the temporal interpolation is [only](#) concerned with the value from the exact (i,j) cell [but](#) and from dates $D-1$ and $D+1$. This ensures that the interpolation will be efficient in the two following extreme scenarios: 1) In a region where we never have satellite observations e.g. the data coverage gap near the North Pole, the spatial interpolation term will be the only contribution. 2) Conversely, in the case of several missing swaths on day D only (nominal coverage on $D-1$ and $D+1$), the interpolated values will be computed from the previous and next days, taking advantage of the persistence of sea ice concentration over relatively short periods. The interpolation for intermediate cases (when both spatial and temporal neighbors exist) is a compromise of those extreme situations.

For the SMMR which was operated every second day, the temporal interpolation is $D-2$ and $D+2$ instead of $D-1$ and $D+1$ for SSM/I and SSMIS.

3. Results and discussion

We compared the ESICR to sea ice charts for reference during the period from Oct. 1978 to Apr. 2015 on both hemispheres. There is a gap in the comparison on the [Southern Hemisphere because we did not have access to ice charts southern hemisphere](#) between 1994 and 2006; [\(see sect. 1.5\)](#). The overlap period during July and August 1987 between the SMMR and the SSM/I instruments [will be](#) analyzed in more detail in section 3.2.

The ice charts are produced to support ship and offshore operations and not to monitor sea ice as a climate parameter. However, [it does they do](#) well in identifying areas of open water and ice and the comparison does in fact reveal trends in the ESICR noise levels.

3.1 The ice concentration comparison to sea ice charts

The NIC ice charts and the ESICR are gridded onto the 12.5 km EASE grid and compared [pixel by pixel](#). The total concentration in the ice chart is given as [the average of the](#) range of sea ice concentrations, [e.g. 10 % to 30 %](#), describing the variability within each ice chart polygon. The bias and STD between ice chart and the ice concentration is computed for ice (ice chart concentration greater than 0%) and for open water (ice chart concentration equal to zero). [The bias in ice concentration between the Northern Hemisphere NIC ice charts and ESICR ice concentration is shown in Figure 4.](#) The ESICR ice concentration is higher than the ice chart over open water by 5 [to 15%.](#) [to 15 % on the northern hemisphere \(Fig. 4\)](#). This is due to the fact that the radiometer ice concentration is affected by atmospheric noise and smearing near the ice edge which increases the ESICR ice concentration above zero. [The while the](#) ice charts have a nominal value of zero over open water. Actually the mean open water ESICR ice concentration is zero at swath level (level 2). However, all negative ice concentration estimates are truncated to zero which leaves the small positive bias in the final product [\(Level level 4\)](#). The uncorrected noise from, [in particular,](#) cloud liquid water, [but also atmospheric](#) water vapor and wind over open water gives a positive bias in the ESICR ice concentrations. The SMMR to SSM/I transition in 1987 is hardly seen even though the SSM/I 19.35 GHz is affected more by water vapor than the 18.0 GHz SMMR instrument. Apparently not all the noise due to [atmospheric](#) water vapor [in the atmosphere and wind](#) is removed successfully in the [atmospheric brightness temperature](#) correction scheme and there is a trend from the beginning to the end of the comparison This [trend](#) is interpreted as a gradual improvement of the NWP data especially since 2002 where the operational model is used instead of ERA 40. [Trends in the amount of cloud liquid water, which is not included in the Tb correction, could also result in the trend which is seen in Figure 4.](#) The ice bias has a clear seasonal cycle and a negative winter bias around -5% to -15%. [The negative bias is caused by the truncation of the over 100% ice concentrations in ESICR. %.](#) The negative summer sea ice bias is sometimes reaching -20%. [This is caused by anomalous sea ice emissivities during melt, the presence of melt ponds, and perhaps an overestimation of the ice concentrations in the ice chart. %.](#)

Both the standard deviation of open water and ice has a clear seasonal cycle with higher standard deviations during summer than during winter (Fig. 5). [The\) and the](#) standard deviation of open water [is has a](#) decreasing [trend](#) during the latter part of the record. This could be a result of higher quality wind and water vapor data in the recent part of the ERA40 reanalysis and in the operational ECWMF model used since 2002.

There is [also](#) a small positive bias over open water [in on](#) the [Southern Hemisphere southern hemisphere](#)

1 due to the truncation of spurious sub-zero ice concentrations in the ESICR (Fig. 6). ~~The near 100%~~
2 ~~sea~~Over ice, ~~the~~ ESICR and NIC ~~ice~~ chart difference is negative around -10% during Antarctic winter.
3 During the Antarctic summer the difference over ice is near -20%.

4
5 The standard deviation of the difference between the ESICR and the NIC ice charts (Fig. 7) is higher
6 and has more inter-annual variability in Antarctica than in the Arctic except for the ~~comparison over~~
7 open water. ~~The standard deviation of where~~ the difference ~~for the open water case~~ is between 0 and 5
8 % from 2006 onwards.

9 **3.2 The SMMR and SSM/I overlap**

10 The overlap period between SMMR and SSM/I during July and August 1987 is short because 15 days
11 prior and after the actual date ~~is~~are needed in order to establish the tie-points properly. Subtracting 15
12 days in each end of the overlap period leaves only a few days where the tie-points are fully established.
13 ~~Figure 8 and 9 show the overall bias between SMMR and SSM/I including~~For the periods where ~~the~~
14 tie-points are ~~based on less than one month data and not fully developed the tie-points~~ for ~~SMMR and~~
15 ~~for SSM/I cover~~ different ~~time periods, for NH and SH, respectively time periods and they are therefore~~
16 ~~expected to differ~~. On the ~~Northern Hemisphere potential biases~~~~northern hemisphere~~ (Fig 8) the bias ~~is~~
17 ~~below 4 % and this~~ may be due to melt ponds with ~~large~~ diurnal variability ~~in their signatures~~ and the
18 two ~~instruments~~~~instruments'~~ different orbits and ~~data~~ coverage.

19
20 The SMMR and SSM/I overlap period coincides with the ice maximum on the ~~Southern~~
21 ~~Hemisphere~~~~southern hemisphere~~ which is ideal for comparison. ~~However, (Fig. 9) and the~~
22 ~~comparison bias~~ is ~~limited by even smaller than on~~ the ~~very short overlap just as for the Northern~~
23 ~~Hemisphere~~~~northern hemisphere~~ (less than 2%). Inspecting the differences geographically (~~not~~
24 ~~shown~~) indicates that when environmental conditions have not changed significantly during SMMR
25 and SSM/I passes then the SSM/I is slightly higher over open water while over ice ~~it is close to neutral~~.
26 ~~The open water bias is probably due to the higher sensitivity of the 19.35 GHz channel on SSM/I to~~
27 ~~water vapor than the 18.0 GHz channel on SMMR~~~~the two estimates are close to each others~~.

28 **3.3 Ice chart and ESICR comparison discussion**

29
30 The uncertainties in the NIC sea ice charts ~~is~~are described in Dedrick et al. (2001). ~~A~~Another study of
31 the differences between ice charts from Greenland and Norwegian ice centers ~~covering the same region~~
32 show relatively large (~~up to 30 %~~) discrepancies ~~up to 30% in~~ ice concentration STD of the difference
33 especially at intermediate concentrations (Breivik et al., 2015). Compared to microwave radiometer ice
34 concentrations (the OSISAF operational algorithm in Andersen et al., (2006B)) the ice concentration in
35 Greenland ice charts is systematically about 30% higher at intermediate concentrations. Trials with the
36 ice concentration model described in section 2.5.3 ~~shows~~show that the estimates from most sea ice
37 concentration algorithms including the Bootstrap and the Bristol ~~is 1:1 proportional to agree very well~~
38 ~~with~~ the actual ice concentration and that there are very small differences between the overall response
39 of different algorithms (ice concentration differences < 1% on 1000 km scale not including noise),
40 ~~i.e.~~). The different algorithms ~~thus~~ yield the same ice concentrations given the same ~~tie-points and~~
41 brightness temperature input. We did not find a similar investigation comparing NIC and other
42 overlapping and coincident ice charts. However, we note that the methodology for making the
43 Greenland, Norwegian and NIC ice charts is similar.

44
45 The bias between ice charts and radiometer ice concentrations at intermediate concentrations ~~could, i.e.~~
46 ~~near the ice edge and in the marginal ice zone, can~~ be caused by two effects: 1) ~~the~~ estimated
47 radiometer ice concentrations are lower than real ice concentration for new ice and if the surface is
48 melting or refrozen after melting ~~and both~~. Both new ice and melting refreezing is abundant in regions
49 with intermediate ~~ice~~ concentrations, ~~i.e.~~ and this will thus lead to the radiometer ~~is~~ underestimating the
50 real ice concentration. ~~A hybrid algorithm such as OSISAF mitigates biases due to melting-refreezing~~
51 ~~to some extent but usage of hemispheric tie points cannot account for existing regional differences in~~
52 ~~melt progress~~. 2) The ice ~~charts~~~~charts'~~ ice concentration is a subjective estimate which is made for the
53 safety of navigation and ~~the~~an overestimation of the ice concentration in the ice chart, ~~particularly near~~
54 ~~the ice edge and in the marginal ice zone, might~~ stem from “better-safe-than-sorry” practices within the
55 ice charting community.

56 **3.4.3.4 The ESICR comparison to the NSIDC sea ice index monthly sea ice extent**

57
58 ~~The differences between sea ice climate data records from the same set of satellite microwave~~
59 ~~radiometer data (SMMR, SSM/I and SSMIS) are primarily due to different spatial resolution, land~~

1 masks and land spill over correction methodologies and different ice concentration thresholds for
2 delineating the sea ice extent. The choice of sea ice concentration algorithms and atmospheric
3 correction methods does also influence the sea ice extent estimate (Kern et al., 2014). The NSIDC sea
4 ice extent is using the NASA Team sea ice concentration algorithm and a 15 % threshold for
5 delineating the sea ice extent. The land masks are similar to the ones used in the ESICR. The mean
6 monthly sea ice extent from the NSIDC is shown together with the ESICR in Tab. 3A and 3B for
7 comparison. In the Arctic (Tab. 3A) the differences between the NSIDC and the ESICR data records
8 are small (less than 0.4 mill. km²). On the Southern Hemisphere the differences are up to 1.5 mill. km²
9 (in Dec.). These differences in sea ice extent are due to the different sea ice concentration thresholds
10 which are used for delineating the ice extent in the ESICR (30 %) and the NSIDC (15 %), the different
11 methods for atmospheric correction, the different sea ice concentration algorithms, and the different tie-
12 points which are used for generating the two datasets (Fetterer et al., 2016).

14 **3.5 The ESICR metrics**

15 In the following we are giving examples of the ESICR dataset for estimating sea ice climate statistics
16 and trends. The applied climate period here is the full length of the ESICR. ~~First we show the long term~~
17 ~~trend in sea ice extent and secondly from Oct. 1978 to the trend in open water days in regions covered~~
18 ~~partend of the season by sea ice. The~~2014. We give examples ~~are given~~ for both ~~the northern and the~~
19 ~~southern hemisphere~~hemispheres.

21 ~~Here~~In this context, the sea ice extent is defined as the area covered by sea ice within the ice edge. The
22 ice edge is defined as the 30 % contour ~~and ice~~. Ice concentrations greater than 30 % are considered as
23 ice covered while concentrations less than 30 % are considered open water. ~~f~~This threshold is higher
24 than e.g. the 15 % threshold used in Parkinson and Cavalieri, (2008) ~~and the igher~~. The higher
25 threshold is needed ~~here~~ because we are not using weather filters in the processing and therefore ~~the~~
26 there ~~is no~~may be more noise over open water ~~resulting in an un-wanted over-estimation of the ice~~
27 ~~extent. The noise level over open water depends on the success of the Tb correction, i.e. partly on the~~
28 ~~quality of the NWP data, and the levels of cloud liquid water, which we cannot yet correct for.~~

29 For the Arctic there is a negative trend in the monthly mean extent for all months of the year. (Tab.

30 3A). The negative slope is largest in September: $-94\,000 \pm 9700 \text{ km}^2/\text{year}^2/\text{yr}^{-1}$ and smallest in May: $-$
31 $32\,000 \pm 4600 \text{ km}^2/\text{yr}$. ~~The monthly trends for the Arctic are shown in Table 3A.~~

32
33
34 $2/\text{yr}^{-1}$. For the Antarctic there is a positive trend in the monthly mean extent for all months of the year.
35 (Tab. 3B). The positive slope is largest in the months April, October and December ~~at~~: $33\,000$
36 $\text{km}^2/\text{year}^2/\text{yr}^{-1}$ and ~~the~~ smallest in February: $13\,000 \pm 5400 \text{ km}^2/\text{yr}$. ~~The monthly trends for the~~
37 ~~Antarctica are shown in Table 3B~~ $2/\text{yr}^{-1}$.

38
39 ~~Below we have looked at two periods of the 35 year ESICR: the entire 35 year period from autumn~~
40 ~~1978 to the end of 2014 and the shorter recent 10 year period from 2004 to the end of 2014. The latter~~
41 ~~shorter period represents the period where most of the~~The mean sea ice extent ~~changes are taking place~~
42 ~~in both the southern and northern hemisphere.~~

43
44 ~~The sea ice extent~~ for the Arctic for ~~both the long and the short record are~~years 1979 through 2014 is
45 shown in Figure 10 together with the September 2012 sea ice extent ~~in Figure 10~~. The lower two
46 panels ~~are showing display~~ the seasonal variability of the sea ice extent and the long term mean monthly
47 sea ice extent in March and in September ~~which is~~, the months with maximum and minimum extent,
48 respectively. ~~In this panel we have included the extent for the most recent 11 years of ESICR (2004 -~~
49 ~~2014) for comparison.~~ September 2012 was the lowest sea ice extent on record in the Arctic since
50 beginning of the satellite era. Over the 35 years of ESICR there is a negative trend in sea ice extent for
51 all months of the year with the largest negative trend during the summer and the beginning of autumn

Formateret: Linjefast: enkelt

Formateret: Linjefast: enkelt

Formateret: Linjefast: enkelt

(Jul-Oct) i.e. the third quarter of the year. - Oct.).

The mean sea ice extent for the Antarctic for ~~both the long and the short record years 1979 through 2014 is shown~~ together with the September 2012 sea ice extent ~~are shown~~ in Figure 11. The lower two panels are showing the seasonal variability of the sea ice extent and the long term mean monthly sea ice extent in March and in September ~~which is the minimum and maximum extent respectively.~~ The sea ice extent has experienced an overall positive trend around Antarctica especially along the ice edge in the Weddell and Ross Seas downstream of the ~~Weddell and the Ross Seas in the clockwise northward branches of the cyclonic~~ atmospheric circulation ~~along the ice edge.~~

In order to ~~determine~~assess the ~~period length~~ of ~~open waters~~the ice season for a given pixel, the annual spatial distribution of dates of freeze-up and break-up were calculated using a simple methodology, yet the results are comparable to Parkinson (2014). The freeze-up date for a given point is defined as the date where the sea ice concentration ~~climbs from below to above~~exceeds 30% and remains so for at least 5 days. ~~The~~Similarly, the break-up date for a given point is defined as the date where the sea ice concentration falls from above to below 30% and remains so for at least 5 days. ~~These thresholds were tested until a reasonable noise level was found.~~

~~The values for the ice concentration threshold and length of period were chosen by manually tuning for convergence: ice concentrations lower than 30% and periods less than 5 days were found to produce noise in the spatial distribution of freeze up/break up dates, which settles at the chosen values, though somewhat less so in the short 10 year record.~~

Since the sea ice does not retreat and expand completely every year, not all areas experience the same number of freeze-ups and break-ups over an equal period of years. Therefore, some regions may experience relatively few freeze-ups and break-ups, thus reducing the confidence in the trend of the region. As a consequence, only areas having experienced more than 6 freeze-ups/break-ups ~~in each period~~ are considered.

~~Figure 12 is showing the decadal trend in open water days in the Arctic region covered by sea ice part of the year.~~The open water days are calculated as the difference in days between freeze-up and break-up:

~~The~~ and the decadal trends in the open water days are shown in Figure 12 for ~~both~~ the long Arctic and the short climate record in Figure ~~12 left and right, respectively~~ 14 for the Antarctic.

~~Over~~In the long Arctic, over the record of 35 years the ice season number of open water days has been ~~shortened~~increasing by at least 60 days in the Davis Strait and in large parts of the Barents Sea. The ice season (the opposite of open water days) has been ~~shortened~~shortening consistently all over the Arctic except in the Bering Strait region and the Greenland Sea- (Fig. 12). The negative trend in the Greenland Sea is not significant and based on an insufficient number of data points. In fact, the large areas with new ice formation which used characterize the ice cover in Greenland Sea has appeared rarely since 2000 (Tonboe and Toudal, 2005; Rogers and Hung, 2008). The shortening of the ice season in the Arctic in general is due both to a delay of the freeze-up and earlier breakup in combination (not shown). This is consistent with e.g. Close et al. (2015). While this pattern is largely consistent for the short and the long periods in the Baffin Bay, and the Barents, Kara and Laptev Seas there are large differences in open water days trend in the Davis Strait and in the Beaufort Sea and Bering Strait region. The short period has substantial negative trends in these regions (more than 15 days / decade) while the long period has positive trends. However, the statistical significance of the trends for the short period is lower than for the long period.

Formateret: Linjeafstand: enkelt

Formateret: Linjeafstand: enkelt

1 The significance of the trends in number of open water days is shown in ~~Figure~~Figures 13 here and 15
2 ~~for the Arctic and Antarctic, respectively~~, as a test of the null-hypothesis, i.e. testing the probability of
3 no trend. This means that a low probability indicates that the trend is in fact significant. It is noted that
4 ~~while the trend is significant in most Arctic regions for the long record the trends are not significant for~~
5 ~~the short record. This (Fig. 13). There is due to the relatively short record of 10 years which is~~
6 ~~influenced by short term natural variability for example shifts in the mean location of the atmospheric~~
7 ~~pressure systems.~~

8
9 ~~Figure 14 shows the a negative~~ decadal trend in the number of open water days around Antarctica in
10 regions with a seasonal sea ice cover. ~~As for (Fig. 14), except in the Arctic-Bellingshausen Sea/
11 Amundsen Sea and the open water days are calculated as the difference in days between freeze-up and
12 breakup.~~

13
14 ~~Indian Ocean.~~ The trend in open water days is shown for both the long and the short record.

15
16 ~~The significance of the trends in number of open water days per year is shown in figure 15 as a test of~~
17 ~~the null hypothesis, i.e. testing the probability of no trend. It is noted that while the trend is significant~~
18 in large regions in the Weddell Sea and in the Ross Sea ~~for the long record the trends are more~~
19 ~~sporadically significant for the short record.~~

20
21 ~~(Fig. 15). The negative trend on in the long record number of open water days in the Ross and in the~~
22 ~~Weddell Seas indicates that the ice is staying longer in these areas now than before. Along the ice edge~~
23 ~~in the Ross Sea, in East Antarctica, the Weddell Sea and in all of the Bellingshausen Sea there is a~~
24 ~~positive trend in the number of open water days. This means that the ice which is either advected into~~
25 ~~or formed in these regions is staying there for shorter time now than before and it indicates that these~~
26 ~~regions have experienced warming during the 35 years of the record. Even though there is an overall~~
27 ~~positive trend in the sea ice extent around Antarctica there is an indication that the warming is closing~~
28 ~~in on Antarctica.~~

29 **4.0 Conclusions**

30 A sea ice climate record covering the period from autumn 1978 to the end of 2014 has been produced
31 based on past satellite microwave radiometer data from SMMR, SSM/I and SSMIS. The climate record
32 has been produced according to 4 principles to ensure consistency and to minimize the sensitivity to
33 noise sources:

34
35
36 1) Finding algorithms with low sensitivities to geophysical noise. Two algorithms have been selected in
37 combination based on the evaluation in Andersen et al., (2007), the Bristol over ice and the Bootstrap
38 in frequency mode over open water. An independent evaluation of algorithms in Ivanova et al. (2015)
39 pointed at the same two algorithms.

Formateret: Linjeafstand: enkelt

1 | 2) Regional error reduction correcting the brightness temperatures for water vapor in the atmosphere
2 | and wind over open water. The scheme described in Andersen et al. (2006B) is used to reduce the noise
3 | over both ice and water.

4 |
5 | 3) Calibrate the algorithms to the actual ice and water signatures and sensor drift using dynamical tie-
6 | points. The result of using dynamical tie-points has been demonstrated here at the transition from
7 | SMMR to SSM/I with satisfactory results. In addition, we do not see any jumps at sensor transitions ~~or~~
8 | ~~long term trends~~ in the comparison to the independent ice chart dataset.

9 |
10 | 4) Quantify the residual uncertainties. A forward model for the residual uncertainties has been
11 | developed and applied. The total uncertainty as a combination of the tie-point variability and the
12 | representativeness uncertainty is a function of the ice concentration and it is applied on each individual
13 | measurement.

14 |
15 | It is clear that the sea ice covers on both hemispheres have undergone large changes over the 35 year
16 | period. In the Arctic the linear trend at sea ice minimum month in September is $-94\ 000\ \text{km}^2\ \text{yr}^{-1}$.

17 |
18 | Around Antarctica there has been an increase of the total sea ice extent during all months especially
19 | downstream of the Weddell Sea and in the Ross Seas. ~~However, these extensions are relatively short~~
20 | ~~lived meaning that the ice which is extending across the long term mean extent (primarily driven by~~
21 | ~~advection) near sea ice extent maximum into the Atlantic and the Pacific ocean is removed by melt or~~
22 | ~~advection relatively quickly.~~ However, there are regional differences and the ice extent has decreased
23 | along the Antarctic Peninsula in the Bellinghausen ~~Sea~~ and the Amundsen Seas.

24 | 4.1 Future work

25 |
26 | The sea ice climate record will be updated at irregular intervals. The next update is planned for autumn
27 | 2016. ~~In addition, the daily OSI SAF sea ice concentration product and the ESICR is using the same~~
28 | ~~algorithm and methodology with only minor differences due to the tie point selection period which is~~
29 | ~~either the last 30 days (operational) or 15 days before and after (reprocessing) It will include~~
30 | ~~development from the ESA sea ice climate change initiative project working towards improved sea ice~~
31 | ~~climate record methodologies (Ivanova et al., 2015).~~

32 |
33 | ~~In addition, the daily near-real-time OSISAF sea ice concentration product and the ESICR are using the~~
34 | ~~same algorithms and similar methodologies. One of the differences is related to the tie-point selection~~
35 | ~~period, which is either the last 30 days (near-real-time) or 15 days before and after (ESICR).~~

36 |
37 | In order to extend the sea ice climate record with past data it is being investigated if it is possible to
38 | retrieve the Nimbus 5 Electrically Scanning Microwave Radiometer (ESMR) 19 GHz swath data from
39 | 1972 to 1977. These single channel data are significantly different from SMMR and SSM/I - SSMIS
40 | data and a new sea ice algorithm would have to be used.

41 |
42 | ~~The next update of the ESICR dataset will include development from the ESA sea ice climate change~~
43 | ~~initiative project working towards improved sea ice climate record methodologies (Ivanova et al.,~~
44 | ~~2015).~~

45 | Acknowledgements

46 | ~~We would like to thank Irene Rubinstein, Walter Meier, and Georg Heygster for their constructive and~~
47 | ~~helpful comments on the manuscript.~~ The work was completed with support from EUMETSAT's
48 | Ocean and Sea Ice Satellite Application Facility. ~~Stefan Kern acknowledges support given by the~~
49 | ~~Center of Excellence for Climate System Analysis and Prediction (CliSAP).~~ The SMMR data were
50 | provided by the NSIDC, the SSM/I data by Remote Sensing Systems, ~~the SSMIS data were processed~~
51 | ~~at NOAA~~ and the numerical weather prediction model data by the ECMWF. ~~We~~ ~~The ice chart data~~ are
52 | ~~grateful for the constructive comments~~ from the ~~three reviewers: Irene Rubinstein, Walter Meier, and~~
53 | ~~Georg Heygster~~ U. S. National Ice Center and NSIDC and the sea ice extent data used for comparison
54 | ~~was provided by the NSIDC.~~
55 |
56 |

Formateret: Linjefast: enkelt

Formateret: Linjefast: enkelt

1 **References** Formateret: Skriftype: Fed

2 Andersen, S. Monthly Arctic sea ice signatures for use in passive microwave algorithms. Danish

3 ~~meteorological institute technical report~~ [Meteorological Institute Technical Report](#) 98-18, 1998, pp. 29,

4 [1998](#).

5

6 Andersen, S., L. Toudal Pedersen, G. Heygster, R. Tonboe, and L. Kaleschke. Intercomparison of Formateret: Linjeafstand: enkelt

7 passive microwave sea ice concentration retrievals over the high concentration Arctic sea ice. *Journal*

8 *of Geophysical Research* 112, C08004, doi:10.1029/2006JC003543, 2007.

9

10 Andersen, S., R. T. Tonboe and L. Kaleschke. Satellite thermal microwave sea ice concentration Formateret: Linjeafstand: enkelt

11 algorithm comparison. *Arctic Sea Ice Thickness: Past, Present and Future*, edited by Wadhams and

12 Amanatidis. *Climate Change and Natural Hazards Series* 10, EUR 22416, 2006A.

13

14 Andersen, S., R. Tonboe, S. Kern, and H. Schyberg. Improved retrieval of sea ice total concentration Formateret: Linjeafstand: enkelt

15 from spaceborne passive microwave observations using Numerical Weather Prediction model fields:

16 An intercomparison of nine algorithms. *Remote Sensing of Environment* 104, 374-392, 2006B.

17

18 Breivik, L.-A. S. Eastwood, J. Karvonen, F. Dinesen, A. Fleming, T. Hamre, L.T. Pedersen, R. Saldo,

19 J.Buus-Hinkler, B. Hackett, F. Arduin, M. B. Jensen. Quality information ~~document~~ [document](#) for Formateret: Linjeafstand: enkelt

20 OSI TAC sea ice products. Issue 1.10, pp. 62. MyOcean ref. MYOF-OSI-QUID-SEAICE, 09. March

21 2015.

22

23 Cavalieri, D. J., C. L. Parkinson. Arctic sea ice variability and trends 1979-2010. *The Cryosphere* 6, Formateret: Linjeafstand: enkelt

24 881-889, 2012.

25

26 Cavalieri, D. J., P. Gloersen, and W. J. Campbell. Determination of Sea Ice Parameters with the Formateret: Linjeafstand: enkelt

27 NIMBUS-7 SMMR. *Journal of Geophysical Research* 89(D4), 5355-5369, 1984.

28

29 Cavalieri, D.J., C.L. Parkinson, P. Gloersen, J.C. Comiso, and H.J. Zwally. Deriving long-term time Formateret: Linjeafstand: enkelt

30 series of sea ice cover from satellite passive-microwave multi-sensor data sets. *Journal of Geophysical*

31 *Research* 104(C7), 15803-15814, 1999.

32

33 Close, S., M.-N. Houssals, C. Herbaut. Regional dependence in the timing of onset of rapid decline in Formateret: Linjeafstand: enkelt

34 Arctic sea ice concentration. ~~JGR~~ [Journal of Geophysical Research - Oceans](#) 120,

35 doi:10.1002/2015JC11187, 2015.

36

37 Comiso J.C, D.J. Cavalieri, C.L. Parkinson, and P. Gloersen. Passive microwave algorithms for sea ice Formateret: Linjeafstand: enkelt

38 concentration: A comparison of two techniques. *Remote Sensing of Environment* 60, 357-384, 1997.

39

40 Comiso J.C. Characteristics of arctic winter sea ice from satellite multispectral microwave Formateret: Linjeafstand: enkelt

41 observations. *Journal of Geophysical Research* 91(C1), 975-994, 1986.

42

43 Comiso, J. C., R. Kwok, S. Martin, A. L. Gordon. Variability and trends in sea ice extent and ice Formateret: Linjeafstand: enkelt

44 production in the Ross Sea. *Journal of Geophysical Research* 116, C04021,

45 doi:10.1029/2010JC006391, 2011.

46

47 Comiso, J. C., R. Kwok, S. Martin, and A. L. Gordon. Variability and trends in sea ice extent and ice Formateret: Linjeafstand: enkelt

48 production in the Ross Sea. *Journal of Geophysical Research* 116, C04021,

1 doi:10.1029/2010JC006391, 2011.

2
3 Dedrick, K. R., K. Partington, M. vanWoert, C. A. Bertoina, D. Benner. U.S. National/Naval Ice Center
4 Digital sea ice data and climatology. Canadian Journal of Remote Sensing 27(5), 457-475, 2001.

Formateret: Linjeafstand: enkelt

6 Drusch, M., E. F. Wood and R. Lindau. The impact of the SSM/I antenna gain function on land surface
7 parameter retrieval. Geophysical Research Letters 26(23), 3481-3484, 1999.

Formateret: Linjeafstand: enkelt

8 ~~Fetterer, F. and Eastwood, S., M. B. Jensen, T. Lavergne, A. M. Sørensen, R. Tonboe. Global Sea Ice~~
9 ~~Concentration Reprocessing. Product User Manual. EUMETSAT OSISAF. Doc. Ver. 2.2. Data ver.~~
10 ~~1.2. Aug. 2015.~~

11 ~~C. Fowler. National Ice Center Arctic sea ice charts and climatology. NSIDC, Boulder, Colorado,~~
12 ~~USA, 2006, updated 2009.~~

Formateret: Linjeafstand: enkelt

14 Fetterer, F. A selection of documentation related to National Ice Center sea ice charts in digital format.
15 NSIDC Special Report # 13, Boulder, Colorado, USA, 2006.

Formateret: Linjeafstand: enkelt

16 ~~Fetterer, F., C. Fowler. National Ice Center Arctic sea ice charts and climatology. NSIDC, Boulder,~~
17 ~~Colorado, USA, 2006, updated 2009.~~

18 ~~Fetterer, F., K. Knowles, W. Meier, M. Savoie. Sea Ice Index, version 2. 1978-2015. Boulder,~~
19 ~~Colorado, USA. NSIDC: National Snow and Ice Data Center. doi:http://dx.doi.org/10.7265/N5736NV7,~~
20 ~~10. Aug., 2016.~~

21 Gloersen, P., and F. T. Barath. A scanning multichannel microwave radiometer for Nimbus-G and
22 SeaSat-A. IEEE Journal of Oceanic Engineering OE-2(2), 172-178, 1977.

Formateret: Linjeafstand: enkelt

24 Gloersen, P., W. J. Campbell, D. J. Cavalieri, J. C. Comiso, C. L. Parkinson, H. J. Zwally. Arctic and
25 Antarctic sea ice, 1978-1987: satellite passive-microwave observations and analysis. NASA SP-511,
26 Washington D. C., 1992.

Formateret: Linjeafstand: enkelt

28 ~~Goosse, H., V. Zunz. Decadal trends in the Antarctic sea ice extent ultimately controlled by ice-ocean~~
29 ~~feedback. The Cryosphere, 8, 453-470, 2014.~~

30 ~~Holland, P. R., R. Kwok. Wind-driven trends in Antarctic sea ice drift. Nature Geoscience 5, 872-875,~~
31 ~~2012.~~

32 Hollinger, J. P., J. L. Peirce, G. A. Poe. 1990. SSM/I instrument evaluation. IEEE Transactions on
33 Geoscience and Remote Sensing 28(5):781-790, 1990.

Formateret: Linjeafstand: enkelt

35 Ivanova, N., Pedersen, L. T., Tonboe, R. T., Kern, S., Heygster, G., Lavergne, T., Sørensen, A., Saldo,
36 R., Dybkjær, G., Brucker, L., and Shokr, M.: Inter-comparison and evaluation of sea ice algorithms:
37 towards further identification of challenges and optimal approach using passive microwave
38 observations, The Cryosphere, 9, 1797-1817, doi:10.5194/tc-9-1797-2015, 2015.

Formateret: Linjeafstand: enkelt

40 ~~Kern, S., F. Bunzel, J. Debernand, H. Heiberg, M. A. Killie, N. Koldunov, T. Lavergne. ESA Sea Ice~~
41 ~~Climate Change Initiative: Phase 1. D4.2 Climate Assessment Report. Doc. Ref.: SICCI-CAR. Version~~
42 ~~1, 26. Nov., 2014.~~

43 Kållberg, P., A. Simmons, S. Uppala, and M. Fuentes. The ERA-40 archive. ERA-40 Project Report
44 Series, ECMWF, Reading, 2004.

Formateret: Linjeafstand: enkelt

46 Meier, W. Scanning Multichannel Microwave radiometer (SMMR) reprocessing for EUMETSAT. OSI
47 SAF Visiting Scientist Report-~~Pp. pp.~~ 9, 2008.

Formateret: Linjeafstand: enkelt

49 ~~Parkinson, C. L., and D. Parkinson, C. L. Spatially mapped reductions in the length of the Arctic sea ice~~
50 ~~season. Geophysical Research Letters 41(12), 4316-4322, 2014.~~

51 ~~Parkinson, C. L., D. J. Cavalieri. Arctic sea ice variability and trends, 1979-2006, Journal of~~

Formateret: Linjeafstand: enkelt

1 Geophysical Research - Oceans, 113, C07003, doi:10.1029/2007JC004558, pp. 28, 2008.
2

3 Poe, G. ~~et al.~~, E.A. Uliana, B.A. Gardiner, T. E. vonRentzell, D. B. Kunkee. Geolocation error analysis
4 of the ~~special sensor microwave imager/sounder~~ Special Sensor Microwave Imager/Sounder. IEEE
5 ~~Trans. Geosci. Rem. Sens.~~ Transactions on Geoscience and Remote Sensing 46(4), 913-922, 2008.
6 Rayner, N. A., D. E. Parker, E. B. Horton, C. K. Folland, L.V. Alexander, D. P. Rowell, E. C. Kent,
7 and A. Kaplan. Global analysis of sea surface temperature, sea ice, and night marine air temperature
8 since the late nineteenth century. Journal of Geophysical Research. 108 (D14).
9 doi:10.1029/2002JD002670, 2003.
10

11 Rogers, J. C. and M.-P. Hung. The Odden ice feature of the Greenland Sea and its association with
12 atmospheric pressure, wind, and surface flux variability from reanalyses. Geophysical Research Letters
13 35, L08504, doi:10.1029/2007GL032938, 2008.
14 Smith, D. M. Extraction of winter sea ice concentration in the Greenland and Barents Seas from SSM/I
15 data. International Journal of Remote Sensing 17(13), 2625-2646, 1996.
16

17 Tonboe, R., R.-H. Pfeiffer, and M. B. Jensen, E. Howe, and S. Eastwood. Validation report for Global
18 sea ice concentration reprocessing. EUMETSAT OSISAF Products OSI-409, Osi-409a, OSI-430. V.
19 2.0, pp. 30. April 2015.
20

21 Tonboe, R. and L. Toudal. Classification of new-ice in the Greenland Sea using Satellite SSM/I
22 radiometer and SeaWinds scatterometer data and comparison with ice model. Remote Sensing of
23 Environment 97, 277-287, 2005.
24 Wentz, F. J. A model function for ocean microwave brightness temperatures. Journal of Geophysical
25 Research 88(C3), 1892-1908, 1983.
26

27 Wentz, F. J. A well-calibrated ocean algorithm for SSM/I. Journal of Geophysical Research 102(C4),
28 8703-8718, 1997.
29

30 Wentz, F. J. User's Manual, SSM/I Antenna Temperature Tapes, Revision 1. RSS Technical Report
31 120191, 1991.
32

33 Wentz, F. J. User's Manual, SSM/I Antenna Temperature Tapes, Revision 2. RSS Technical Report
34 120193, 1993.
35

36 Wentz, F. J. User's Manual, SSM/I Antenna Temperature, Version 6. *RSS Technical Memo 082806*,
37 2006.
38

39 Wentz, F. J., L. Ricciardulli, K. Hilburn, C. Mears. How much more rain will global warming bring?
40 Science 10.1126/science.1140746, 2007.
41

42 Zhang, X. D., and J. E. Walsh. Toward a seasonally ice-covered Arctic Ocean: Scenarios from the
43 IPCC AR4 model simulations. Journal of Climate, 19(9), 1730-1747, 2006.
44

1
2 **Tables**

3
4
5 ~~Table 1. The different satellite missions carrying the SMMR, SSM/I and SSMIS instrument and the~~
6 ~~periods they cover.~~

7
8 ~~Table 2. The STD of the difference between the simulated SSM/I—SSMIS satellite ice concentration~~
9 ~~and the reference ice concentration resampled to different grid resolutions in percent.~~

10
11 ~~Table 3A. The mean monthly sea ice extent, long term trend and standard error of the trend in the~~
12 ~~Arctic. All figures are in millions of km².~~

13
14 ~~Table 3B. The mean monthly sea ice extent, long term trend and standard error of the trend in the~~
15 ~~Arctic. All figures are in millions of km².~~

← **Formateret:** Linjeafstand: enkelt

16
17

Sensor	Launch	End
Nimbus 7 SMMR	October 1978	August 1987
DMSP F8 SSM/I	June 1987	December 1991
DMSP F10 SSM/I	December 1990	November 1997
DMSP F11 SSM/I	November 1991	May 2000
DMSP F13 SSM/I	March 1995	November 2009
DMSP F14 SSM/I	May 1997	August 2008
DMSP F15 SSM/I	December 1999	-
DMSP F16 SSMIS	October 2003	-
DMSP F17 SSMIS	November 2006	-
DMSP F18 SSMIS	October 2009	-
DMSP F19 SSMIS	April 2014	-

18 Table 1. The ~~different~~ satellite missions carrying the SMMR, SSM/I and SSMIS instrument and the
19 periods they cover.
20

21

	1 km	5 km	10 km	12 km	25 km	50 km
CF	18	16	14	13	10	7
Bristol	17	15	13	12	10	6
OSISAF	17	15	13	12	9	6

22 Table 2. The STD of the difference between the simulated SSM/I - SSMIS satellite ice concentration
23 and the reference ice concentration resampled to different grid resolutions in percent.

Month	Mean [10 ⁶ km ²]	Trend [10 ⁶]	Trend std err [10 ⁶]	NSIDC Sea Ice

← **Formateret tabel**

← **Indsatte celler**

		km ² yr ⁻¹]	km ² yr ⁻¹]	Index mean [10 ⁶ km ²]
Jan January	14.641	-0.045	0.0040	<u>14.589</u>
Feb February	15.505	-0.045	0.0043	<u>15.407</u>
March Mar	15.620	-0.041	0.0042	<u>15.572</u>
Apr April	14.772	-0.036	0.0048	<u>14.838</u>
May	13.403	-0.032	0.0046	<u>13.434</u>
Jun June	11.899	-0.053	0.0044	<u>11.908</u>
Jul July	09.667	-0.079	0.0060	<u>09.641</u>
August Aug	07.458	-0.084	0.0083	<u>07.144</u>
September Sep	06.881	-0.094	0.0097	<u>06.395</u>
October Oct	09.053	-0.077	0.0089	<u>08.821</u>
Nov November	11.138	-0.055	0.0052	<u>10.983</u>
Dec December	13.241	-0.044	0.0043	<u>13.107</u>

Formateret: Dansk

Formateret: Dansk

Formateret: Dansk

Formateret: Dansk

1 Table 3A. The mean monthly sea ice extent 1978 - 2014, long term trend and standard error of the
 2 trend in the Arctic. All figures are in millions of km². The right hand column is showing the mean
 3 monthly NSIDC sea ice index Arctic sea ice extent (1978 - 2014) for comparison (Fetterer et al., 2016).
 4

Month	Mean [10 ⁶ km ²]	Trend [10 ⁶ km ² yr ⁻¹]	Trend std err [10 ⁶ km ² yr ⁻¹]	NSIDC Sea Ice Index mean [10 ⁶ km ²]
Jan January	04.566	0.022	0.0092	<u>05.295</u>
Feb February	02.911	0.013	0.0054	<u>03.148</u>
March Mar	04.105	0.022	0.0072	<u>04.461</u>
Apr April	06.860	0.033	0.0099	<u>07.459</u>
May	10.135	0.032	0.0089	<u>10.843</u>
Jun June	13.229	0.029	0.0072	<u>14.018</u>
Jul July	15.622	0.022	0.0055	<u>16.523</u>
Aug August	17.129	0.022	0.0059	<u>18.214</u>
September Sep	17.684	0.029	0.0089	<u>18.909</u>
Oct October	17.278	0.033	0.0070	<u>18.460</u>
Nov November	15.164	0.020	0.0065	<u>16.388</u>
Dec December	09.932	0.033	0.0115	<u>11.412</u>

Formateret tabel
 Indsatte celler

Formateret: Dansk

Formateret: Dansk

5 Table 3B. The mean monthly sea ice extent, long term 1978 - 2014, trend and standard error of the
 6 trend in the Arctic Antarctic. All figures are in millions of km². The right hand column is showing the

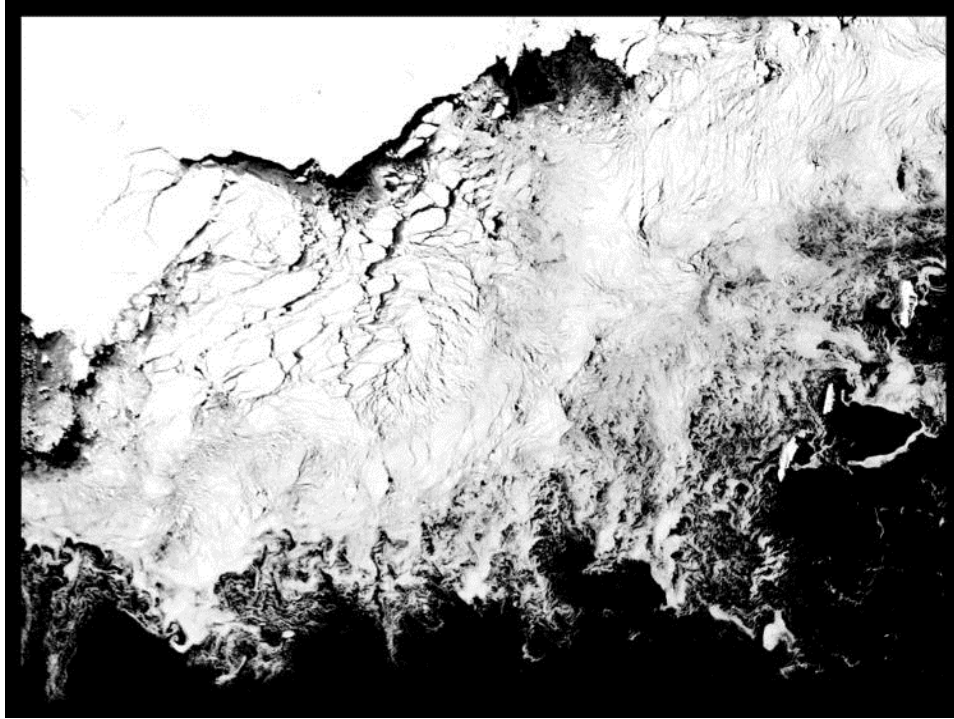
1 | [mean monthly NSIDC sea ice index Antarctic sea ice extent \(1978 - 2014\) for comparison \(Fetterer et](#)
2 | [al., 2016\).](#)
3

1
2
3
4

Figures

Captions:

Formateret: Skrifttype: Ikke Fed



5
6
7
8
9
10
11

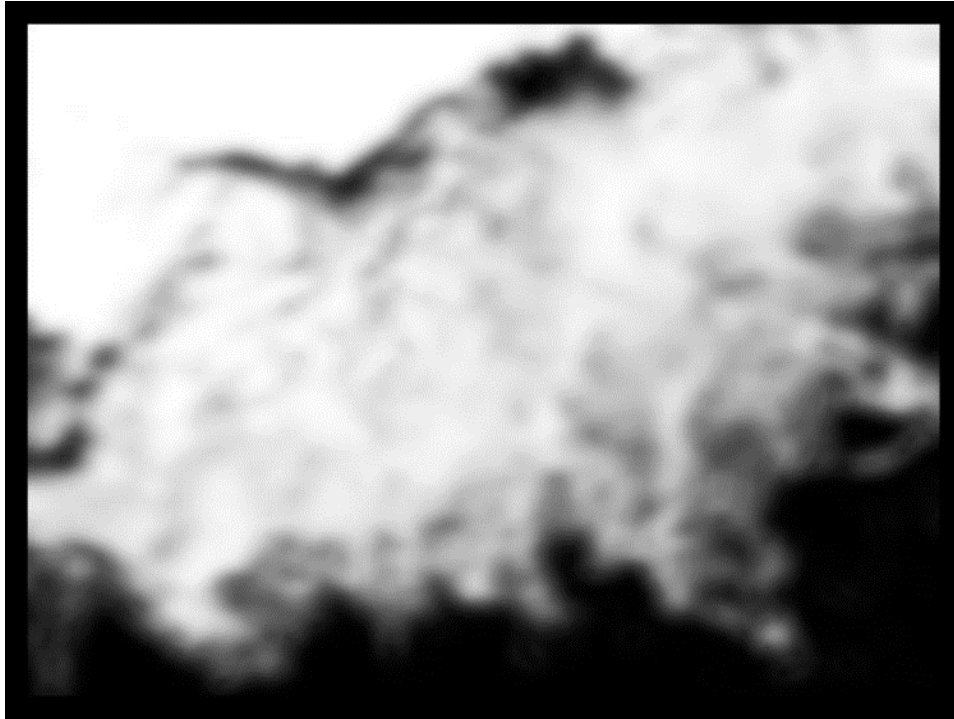
Figure 1. The 1 km cloud free MODIS image 3000 x 2200 km. The scene is situated north of McMurdo Station and east of the Ross Sea, Antarctica. Ice concentrations between 0.% (black) and 100.% (white). The scene is recorded at 03.30 UTC 2008/02/24 by the Aqua satellite. The scene ~~center~~centre is at ~~69.5S, 165W~~5°S, 165°W.

Formateret: Linjeafstand: enkelt

Formateret: Dansk

Formateret: Dansk

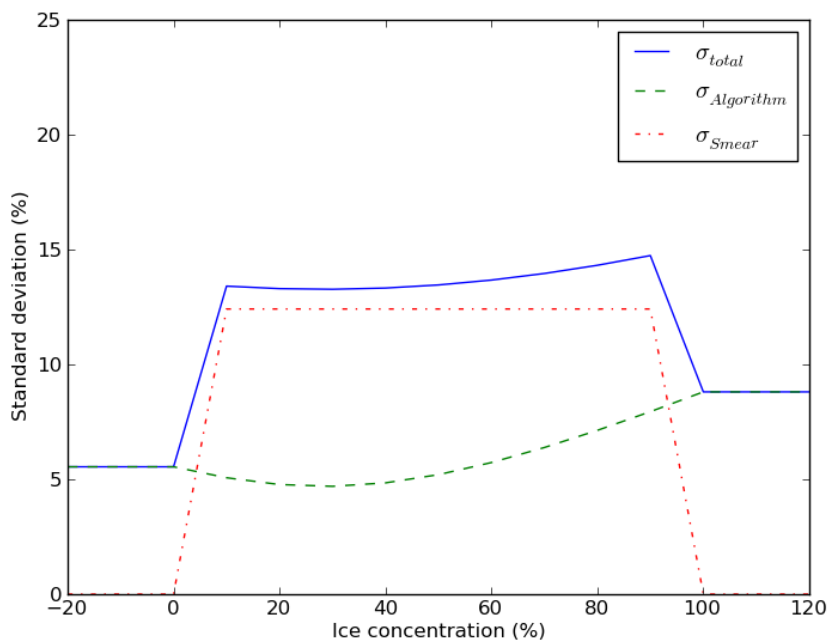
Formateret: Dansk



1
2
3
4
5

Figure 2. The simulated ice concentrations using the SSM/I sensor specifications and the OSI SAF OSISAF hybrid ice concentration algorithm and the data in figure 1 as input. Ice concentrations between 0% (black) and 100% (white).

Formateret: Linjeafstand: enkelt



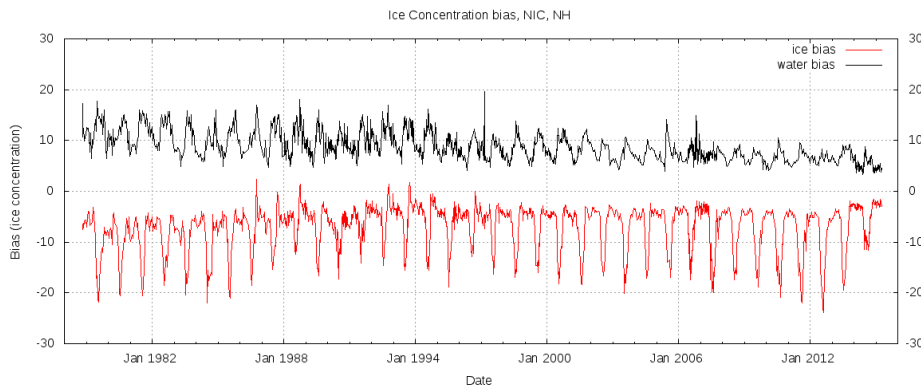
Formateret: Linjeafstand: enkelt

Formateret: Dansk

6
7
8

Figure 3. The total uncertainty in blue and its two components: the smearing uncertainty in red and the tie-point uncertainty in green as a function of ice concentration.

1



Formateret: Dansk
 Formateret: Linjeafstand: enkelt

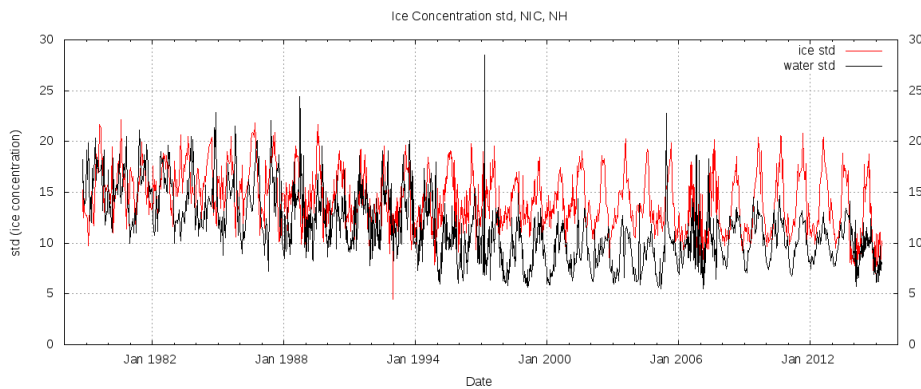
2

Figure 4. The Arctic ESICR - NIC ice chart mean difference (bias) for areas of ice in red, and for areas of open water in black and the total, i.e. both ice and water, in blue.

3

4

5



Formateret: Dansk
 Formateret: Linjeafstand: enkelt

6

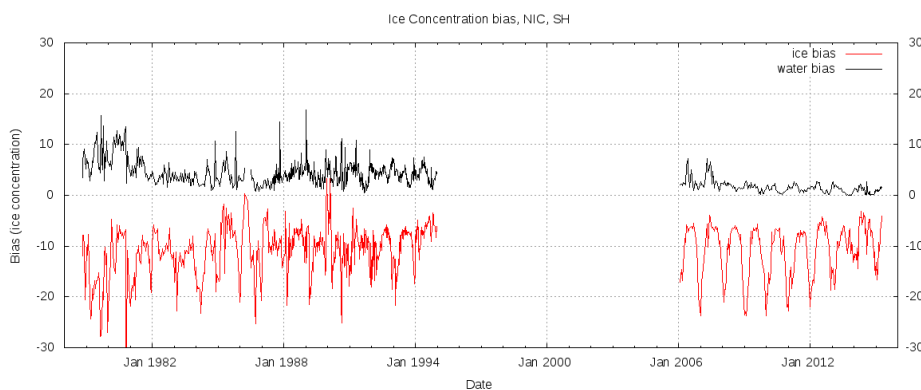
Figure 5. The Arctic ESICR - NIC ice chart standard deviation of the difference for areas of ice in red, and for areas of open water in black and the total, i.e. both ice and water, in blue.

7

8

9

10



Formateret: Linjeafstand: enkelt

11

12

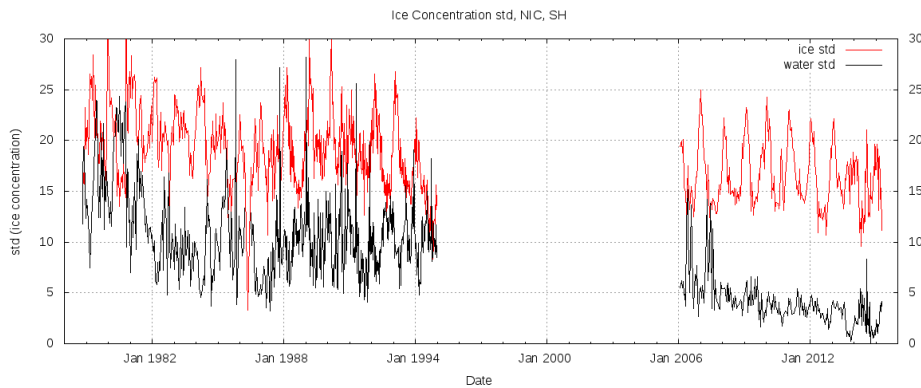
13

14

15

Figure 6. The Antarctic ESICR - NIC ice chart mean difference (bias) for areas of ice in red, and for areas of open water in black and the total, i.e. both. No ice and water, in blue charts were available to us from 1994 to 2006.

1



2

3

4

5

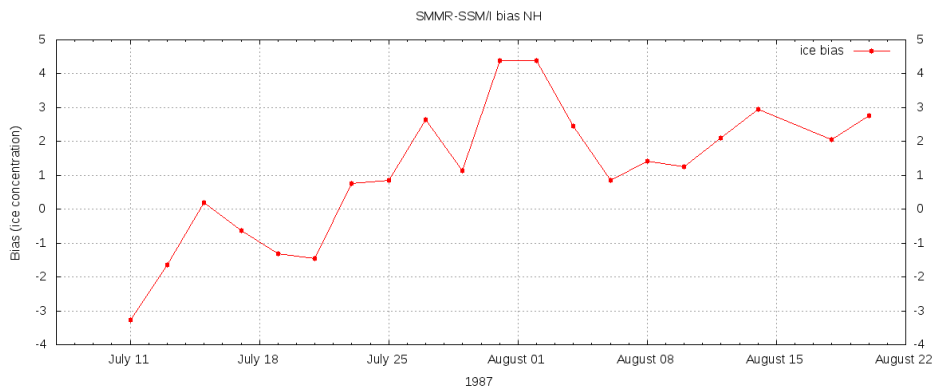
6

7

Figure 7. The ESICR and NIC ice chart standard deviation of the difference around Antarctica. ~~The blue curve is showing the total standard deviation of the difference for both areas of open water and ice.~~ The red curve is for ice and the black curve is for water. No ice charts were available to us from 1994 to ~~2003~~2006.

Formateret: Linjeafstand: enkelt

8



9

10

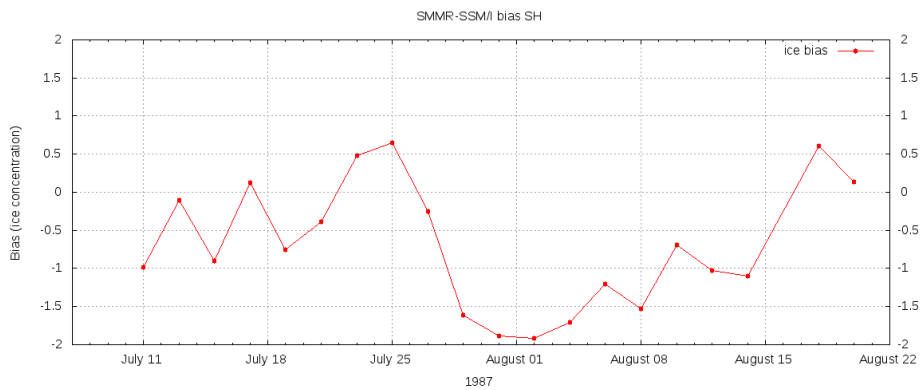
11

12

Figure 8. The overlapping SMMR - SSM/I difference in the Arctic during summer melt. ~~The blue curve is the total bias and the~~The red curve is showing the ice bias.

Formateret: Linjeafstand: enkelt

13



14

15

Figure 9. The overlapping SMMR - SSM/I difference around Antarctica during austral winter. ~~The blue~~

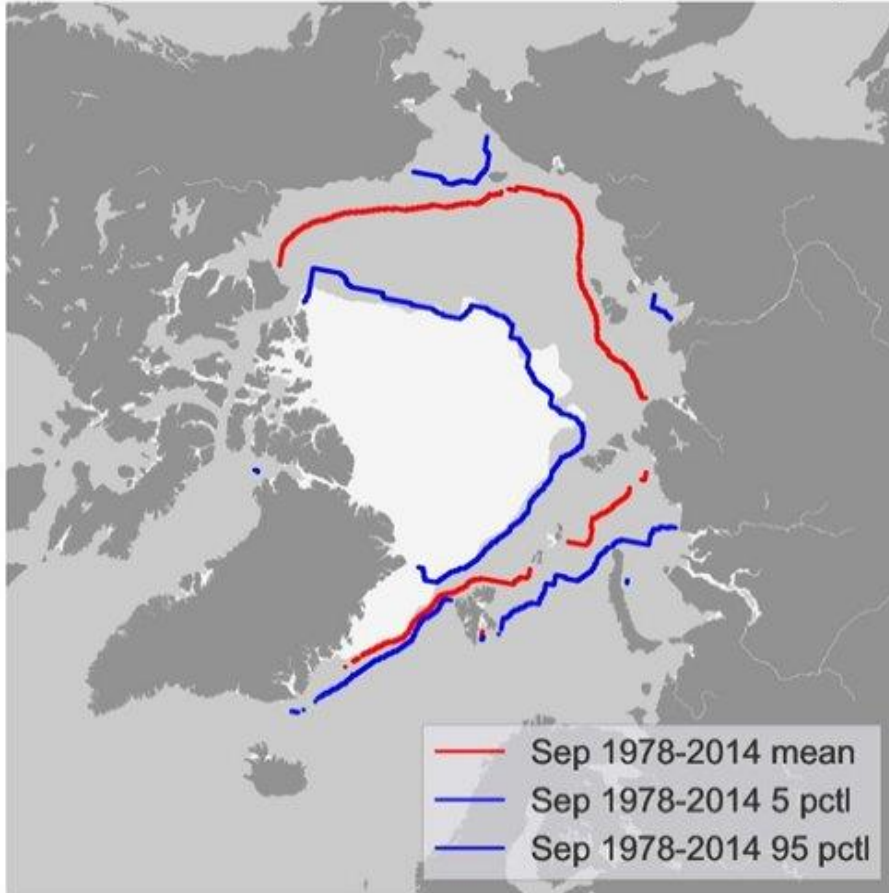
Formateret: Linjeafstand: enkelt

1 curve is the total bias and the red curve is showing the ice bias.

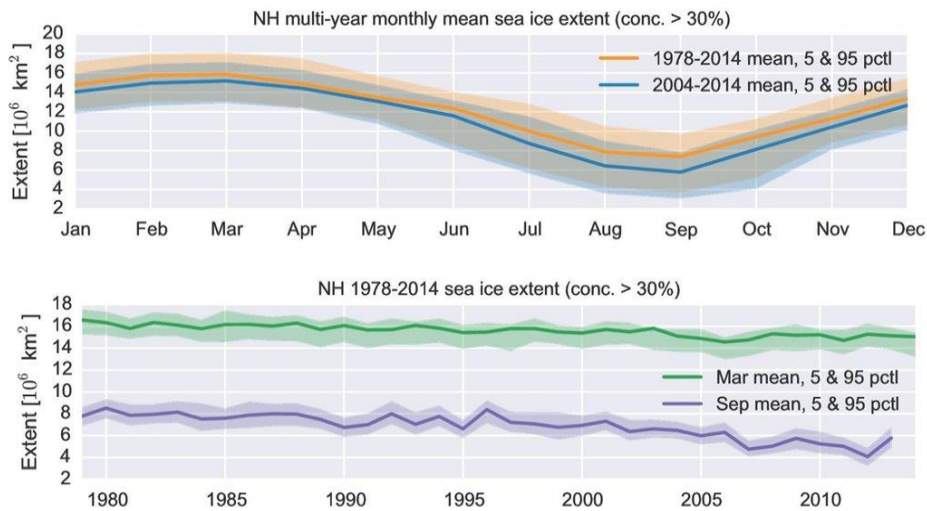
2

3

Sep 2012 versus Sep 1978-2014 (conc. > 30 %)



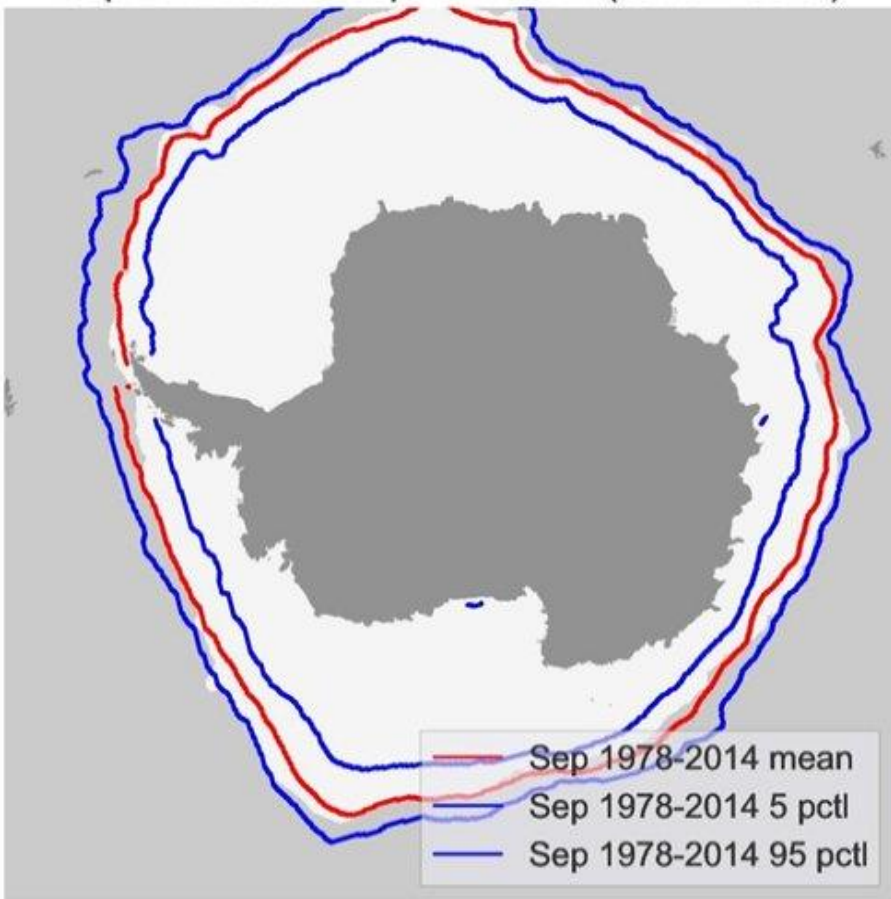
4



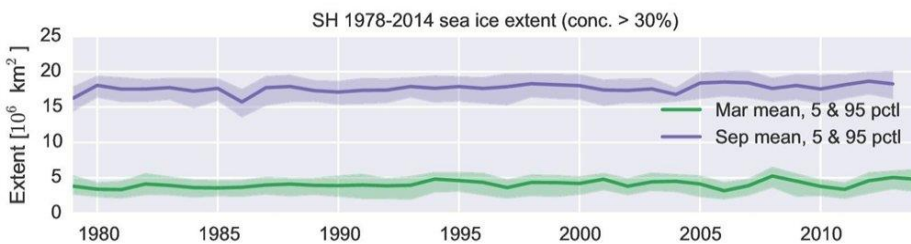
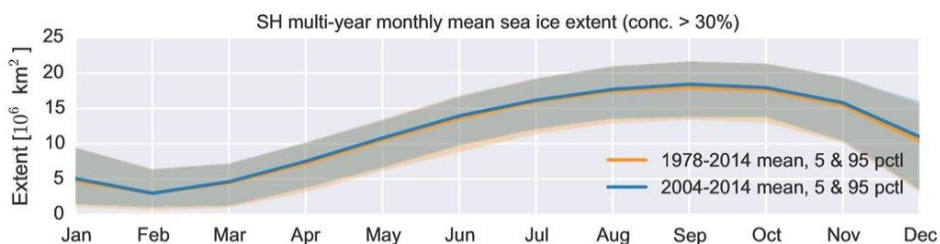
1
 2 Figure 10. The upper panel: the September 2012 sea ice extent in the Arctic compared to the mean
 3 extent **for the long (left) and the short record (right)** shown with the red line. The blue lines on either
 4 side of the mean extent line (red) are the 5 and 95 percentiles of ice extent. The lower two panels are
 5 showing the annual cycle of sea ice extent. The shaded areas are the 5 and 95 % percentiles **of the**
 6 **inter-annual and daily variability, respectively.** The lower panel is showing the long term (1978-
 7 2014) Arctic sea ice extent near its maximum in March and near its minimum in September.
 8
 9

Formateret: Linjeafstand: enkelt

Sep 2012 versus Sep 1978-2014 (conc. > 30 %)



1



2
3

Figure 11. The upper panel: the September 2012 sea ice extent in the Antarctic compared to the mean

1 extent for the long and the short record shown with the red line. The blue lines on either side of the
2 mean extent line are the 5 and 95 percentiles of ice extent. The lower two panels are showing the
3 annual cycle of sea ice extent. The shaded areas are the 5 and 95% percentiles. The lower panel is
4 showing the long term (1978-2014) Antarctic sea ice extent near its maximum in March and near its
5 minimum in September.

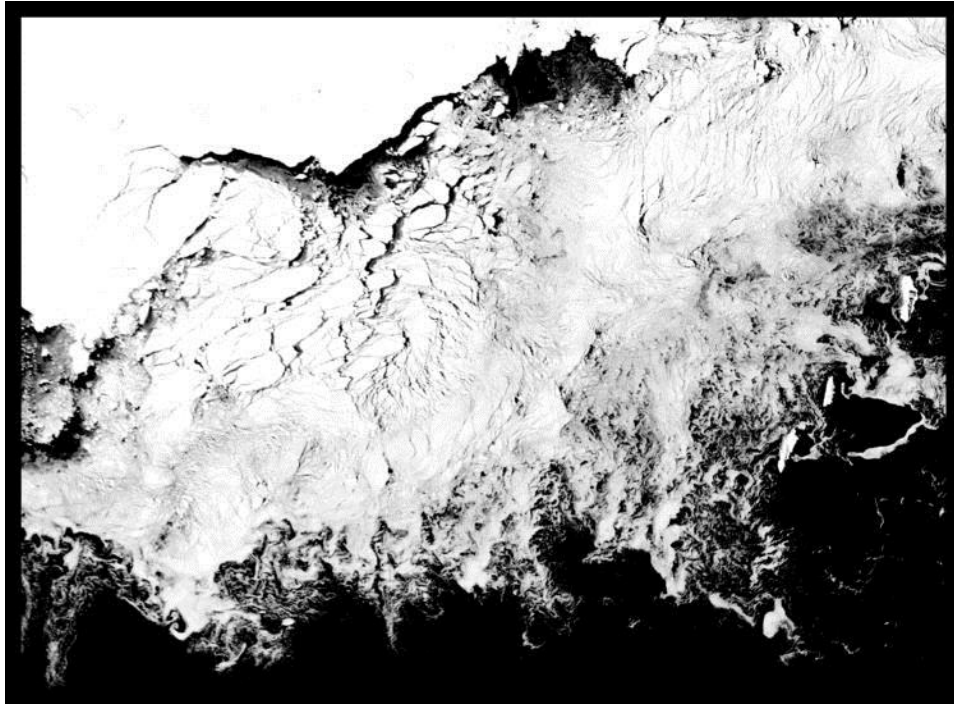
6
7 Figure 12. Show the linear trend in open water days in the Arctic for the long record (1978-2014) to the
8 left and the short record (2004-2014) to the right.

9
10 Figure 13. The probability that the trend in figure 12 is not significant (test of the null hypothesis). A
11 low value (< 5) indicates that the trend is significant.

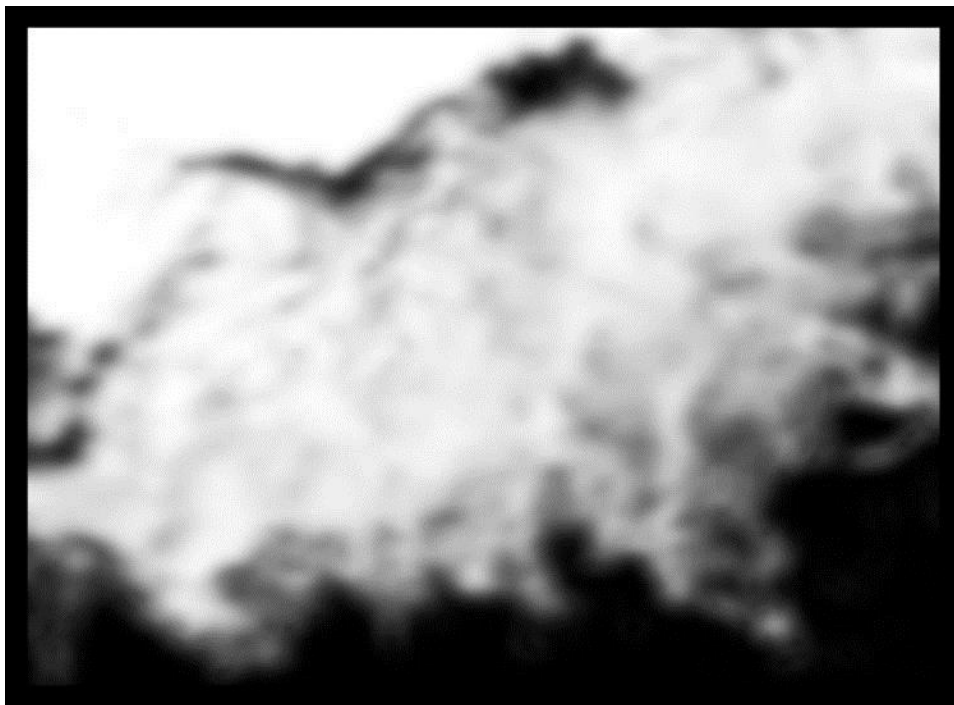
12
13 Figure 14. Show the linear trend in open water days in the Antarctic for the long record (1978-2014) to
14 the left and the short record (2004-2014) to the right.

15
16 Figure 15. The probability that the trend in figure 14 is not significant (test of the null hypothesis). A
17 low value ($< 5\%$) indicates that the trend is in fact significant.

18
19
20



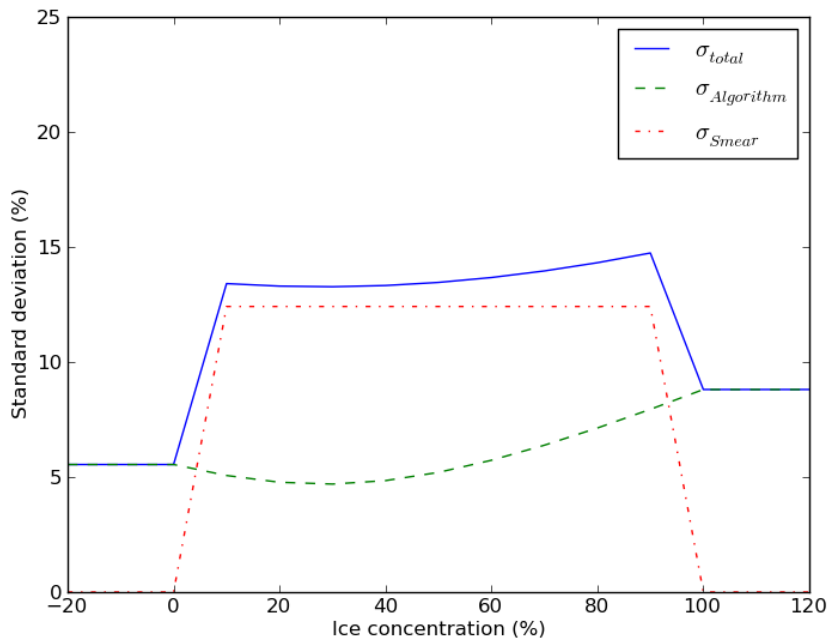
1
2
3
4
5
6
Figure 1. The 1 km cloud-free MODIS image 3000 x 2200 km. The scene is situated north of McMurdo Station and east of the Ross Sea, Antarctica. Ice concentrations between 0% (black) and 100% (white). The scene is recorded at 03.30 UTC 2008/02/24 by the Aqua satellite. The scene centre is at 69.5S, 165W.



7
8
9
Figure 2. The simulated ice concentrations using the SSM/I sensor specifications and the OSI-SAF hybrid ice concentration algorithm and the data in figure 1 as input. Ice concentrations between 0%

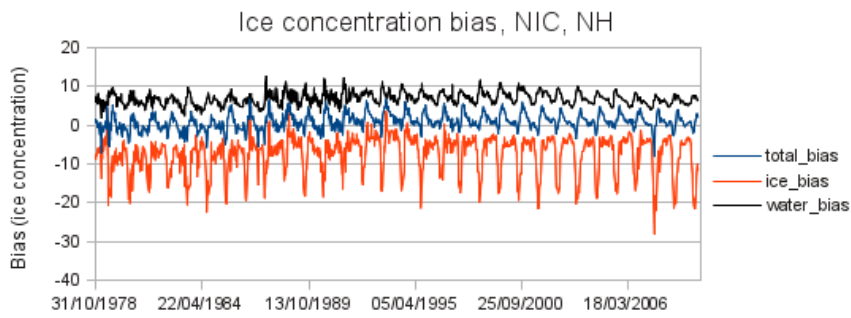
1
2

(black) and 100% (white).



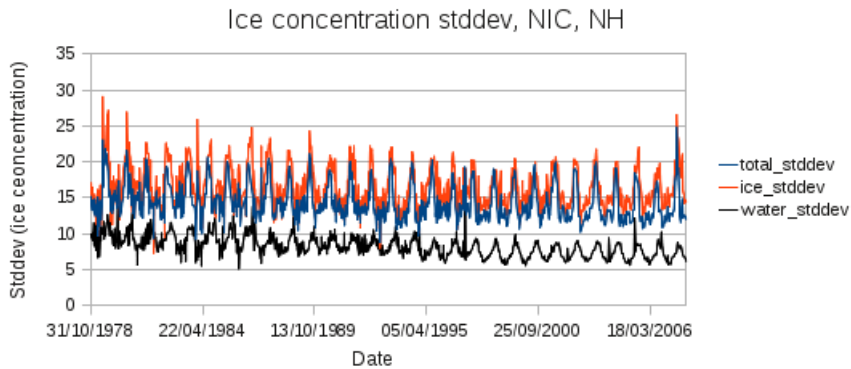
3
4
5
6

Figure 3. The total uncertainty in blue and its two components the smear in red and the tie-point uncertainty in green as a function of ice concentration.

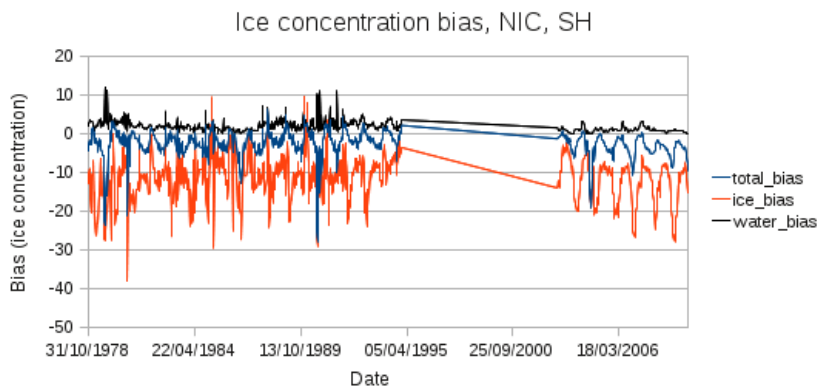


7
8
9
10
11

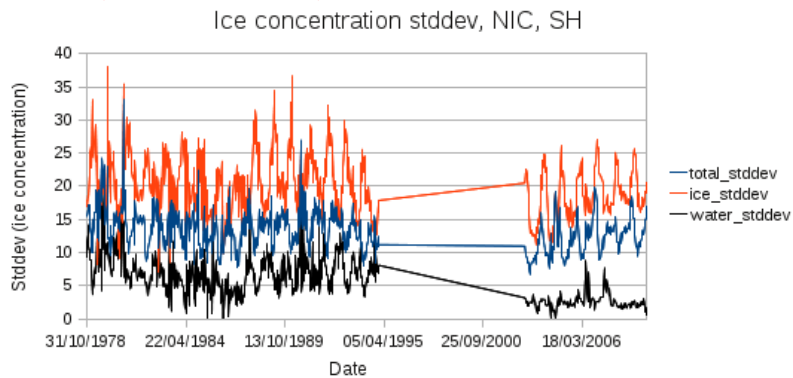
Figure 4. The Arctic ESICR—NIC ice chart difference for areas of ice in red, for areas of open water in black and the total, i.e. both ice and water, in blue.



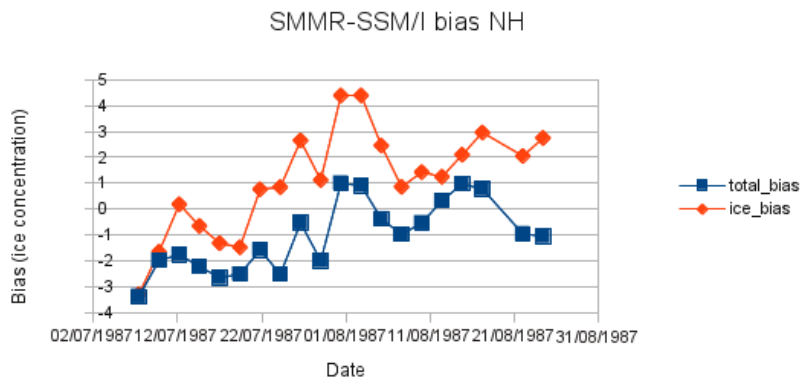
1
2
3
4
5
Figure 5. The Arctic ESICR – NIC ice chart standard deviation of the difference for areas of ice in red, for areas of open water in black and the total, i.e. both ice and water, in blue.



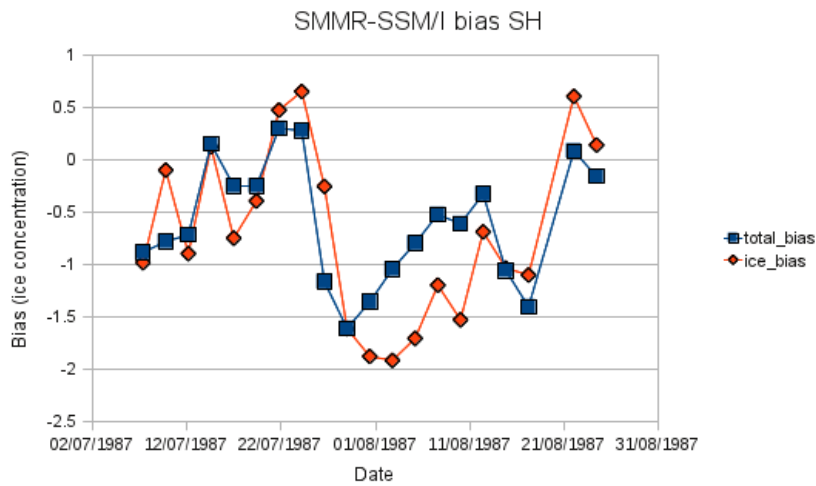
6
7
8
Figure 6. The Antarctic ESICR – NIC ice chart difference for areas of ice in red, for areas of open water in black and the total, i.e. both ice and water, in blue.



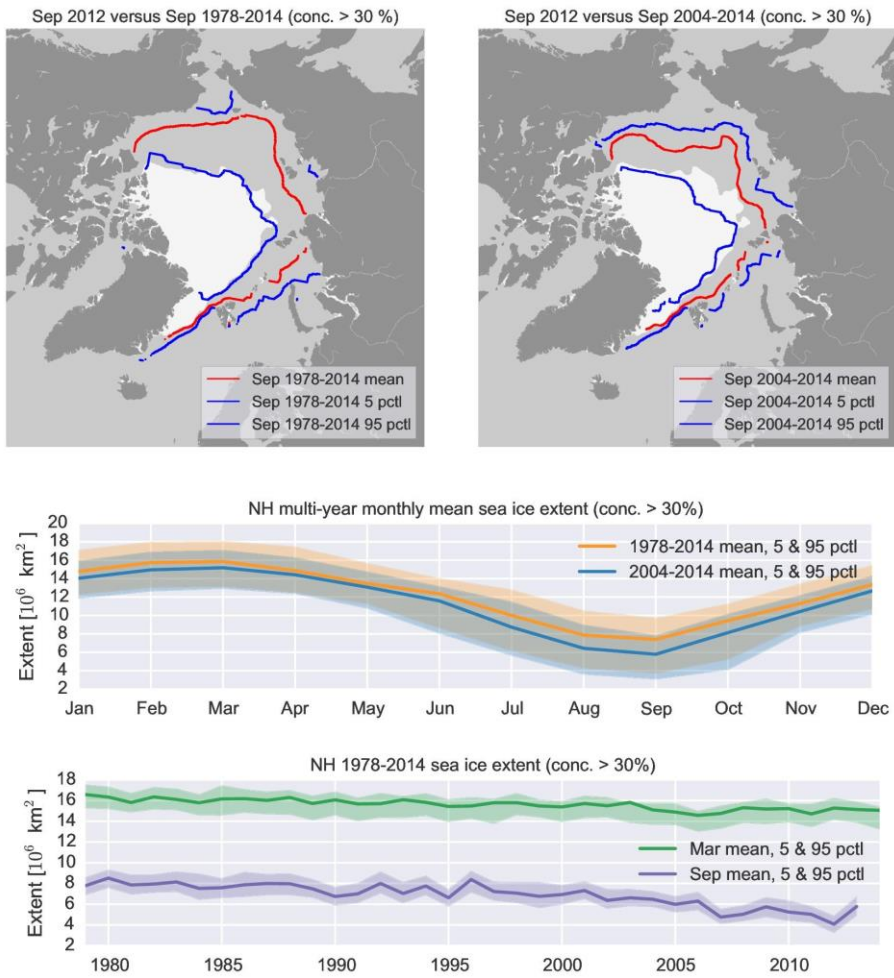
9
10
11
12
13
Figure 7. The ESICR and NIC ice chart standard deviation of the difference around Antarctica. The blue curve is showing the total standard deviation of the difference for both areas of open water and ice. The red curve is for ice and the black curve is for water. No ice charts were available to us from 1994 to 2003.



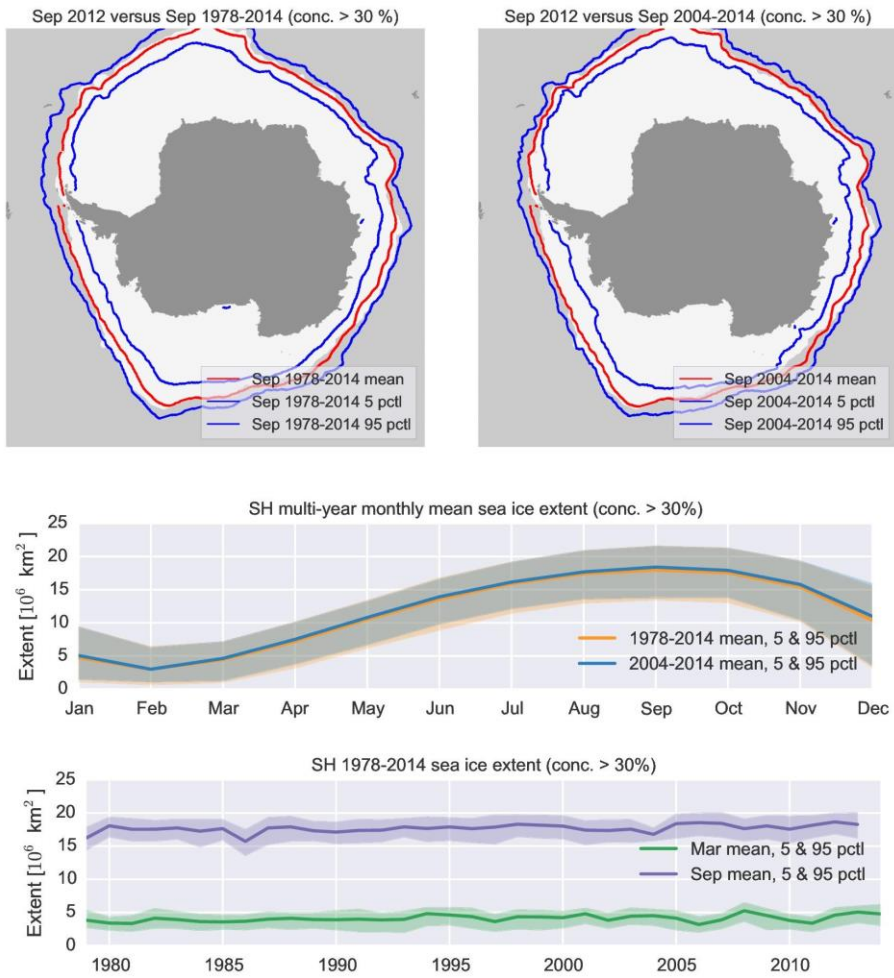
1
2
3
Figure 8. The overlapping SMMR—SSM/I difference in the Arctic during summer melt. The blue curve is the total bias and the red curve is showing the ice bias.



4
5
6
7
Figure 9. The overlapping SMMR—SSM/I difference around Antarctica during austral winter. The blue curve is the total bias and the red curve is showing the ice bias.

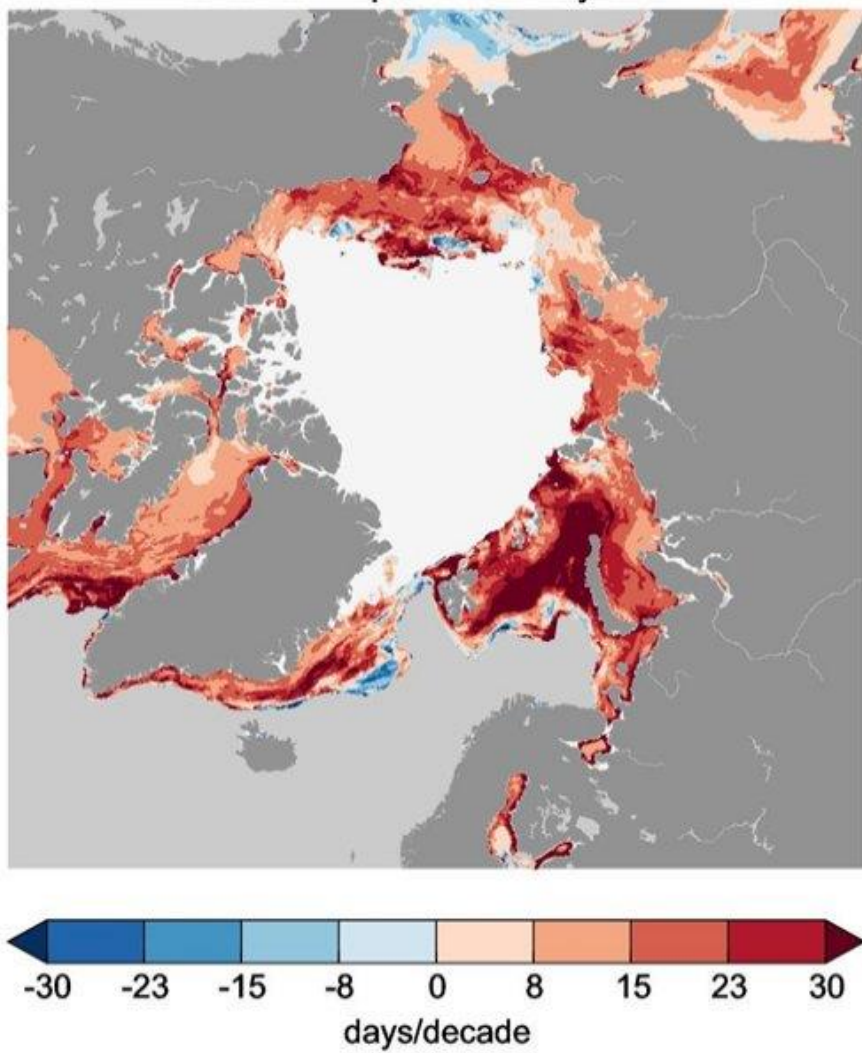


1
2
3
4
5
6
7
8
Figure 10. The upper panel: the September 2012 sea ice extent in the Arctic compared to the mean extent for the long (left) and the short record (right) shown with the red line. The blue lines on either side of the mean extent line are the 5 and 95 percentiles of ice extent. The lower two panels are showing the annual cycle of sea ice extent. The shaded areas are the 5 and 95 % percentiles of the inter-annual and daily variability, respectively. The lower panel is showing the long term (1978–2014) Arctic sea ice extent near its maximum in March and near its minimum in September.



1
2
3
4
5
6
Figure 11. The upper panel: the September 2012 sea ice extent in the Antarctic compared to the mean extent for the long and the short record shown with the red line. The blue lines on either side of the mean extent line are the 5 and 95 percentiles of ice extent. The lower two panels are showing the annual cycle of sea ice extent. The shaded areas are the 5 and 95% percentiles. The lower panel is showing the long term (1978-2014) Antarctic sea ice extent near its maximum in

1978-2014 open water days trend



1
2

~~March and near its minimum in September.~~

Formateret: Dansk

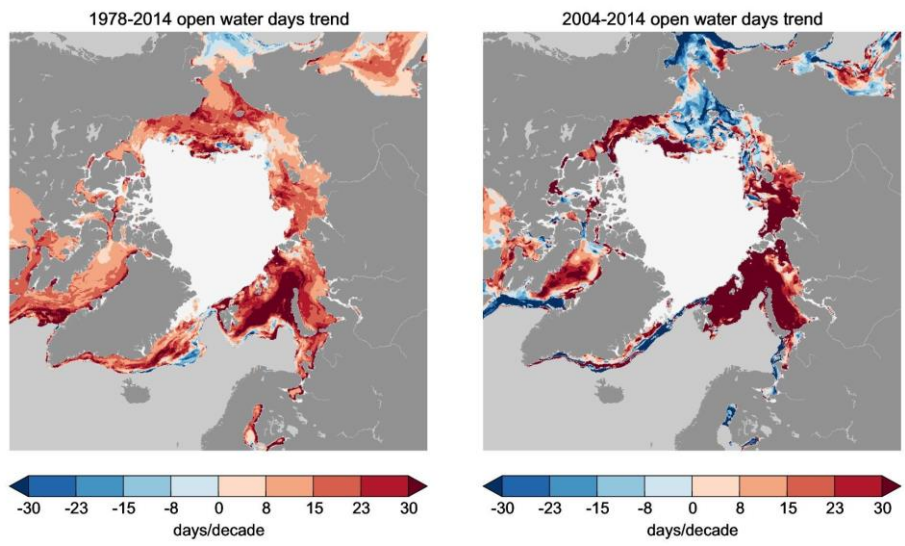
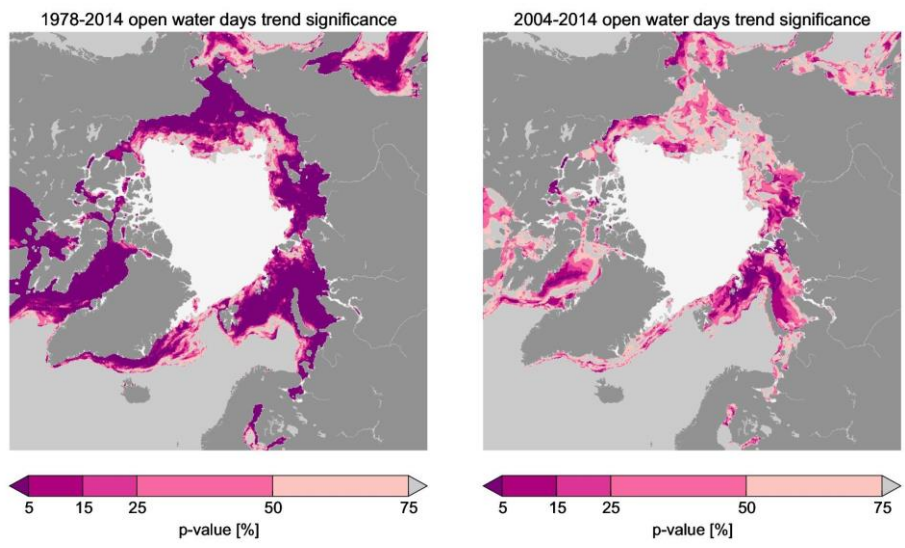


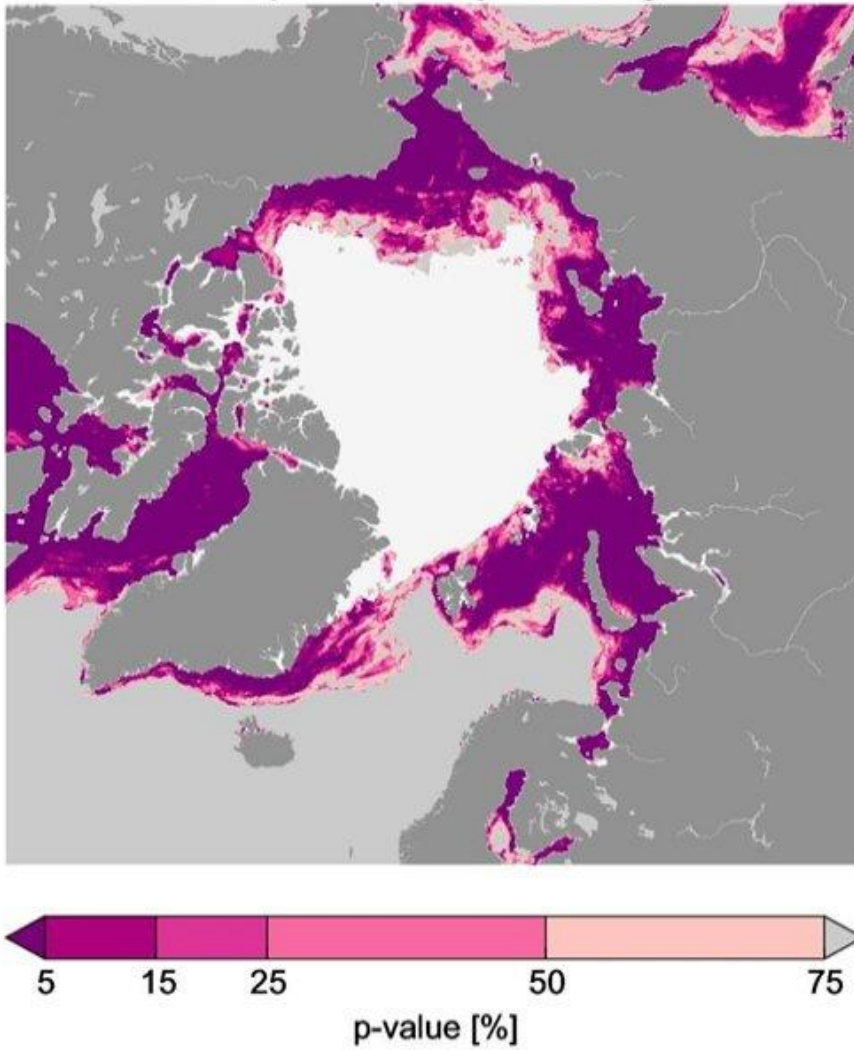
Figure 12. Show the linear trend in open water days in the Arctic for the long record (1978-2014) to the left and the short record (2004-2014) to the right (1978-2014).



1
2
3

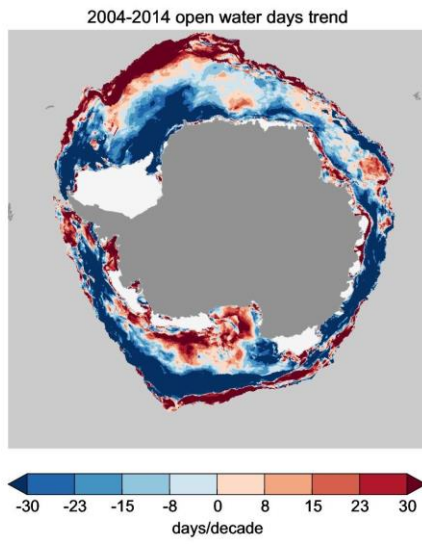
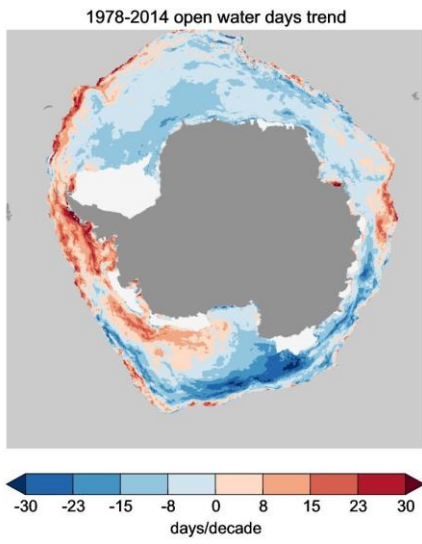
4
5

1978-2014 open water days trend significance

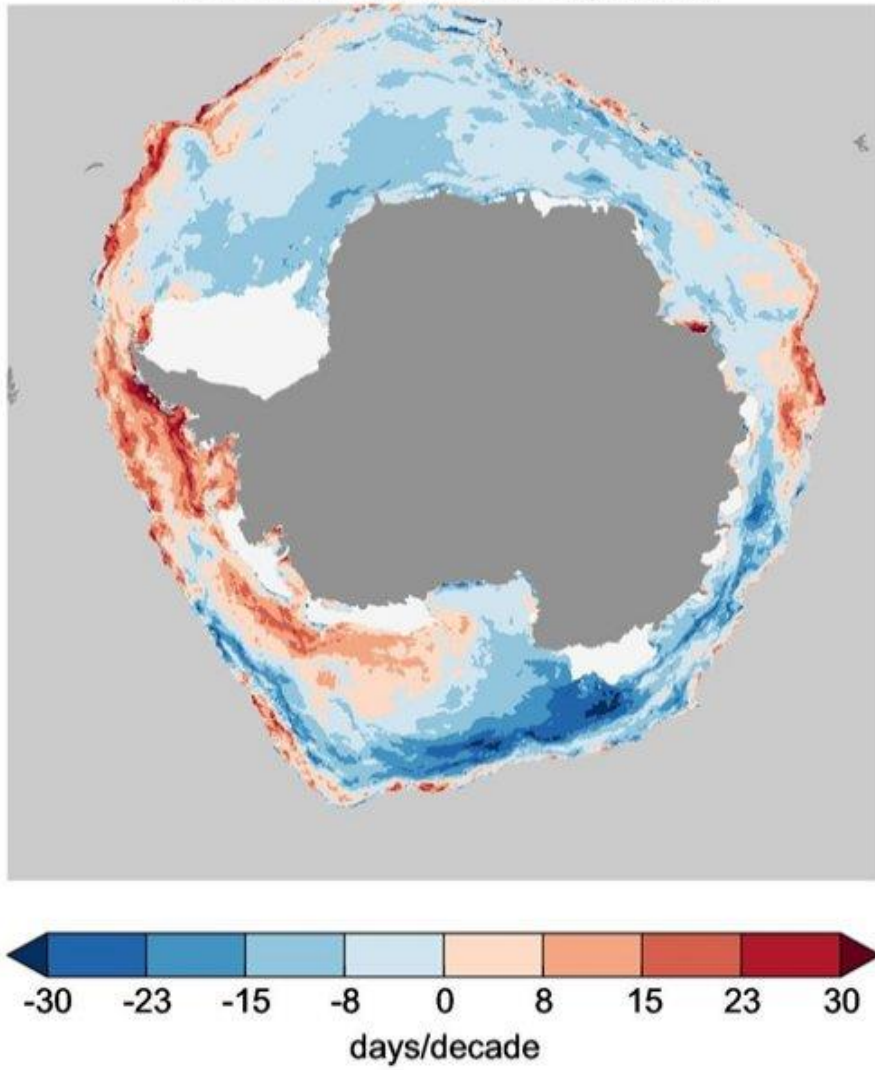


1
2
3

Figure 13. The probability that the trend in [figureFigure 12](#) is not significant (test of the null-hypothesis). A low value (< 5%) indicates that the trend is significant.

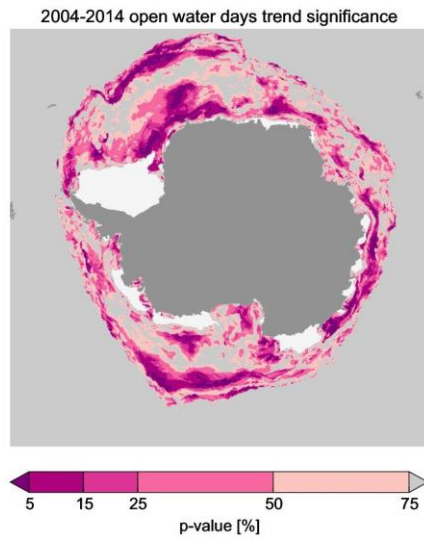
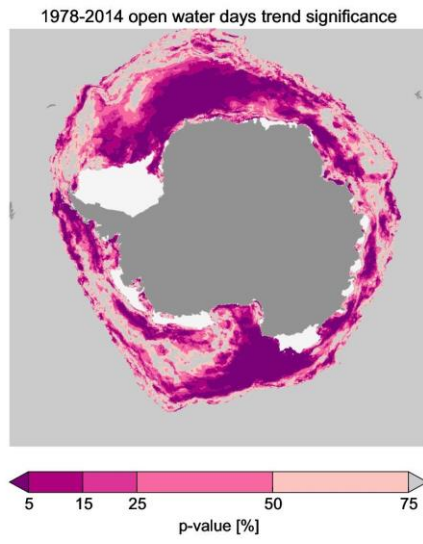


1978-2014 open water days trend



1
2
3

Figure 14. Show the linear trend in open water days in the Antarctic for the long record (1978-2014) to the left and the short record (2004-2014) to the right. (1978-2014).



1978-2014 open water days trend significance

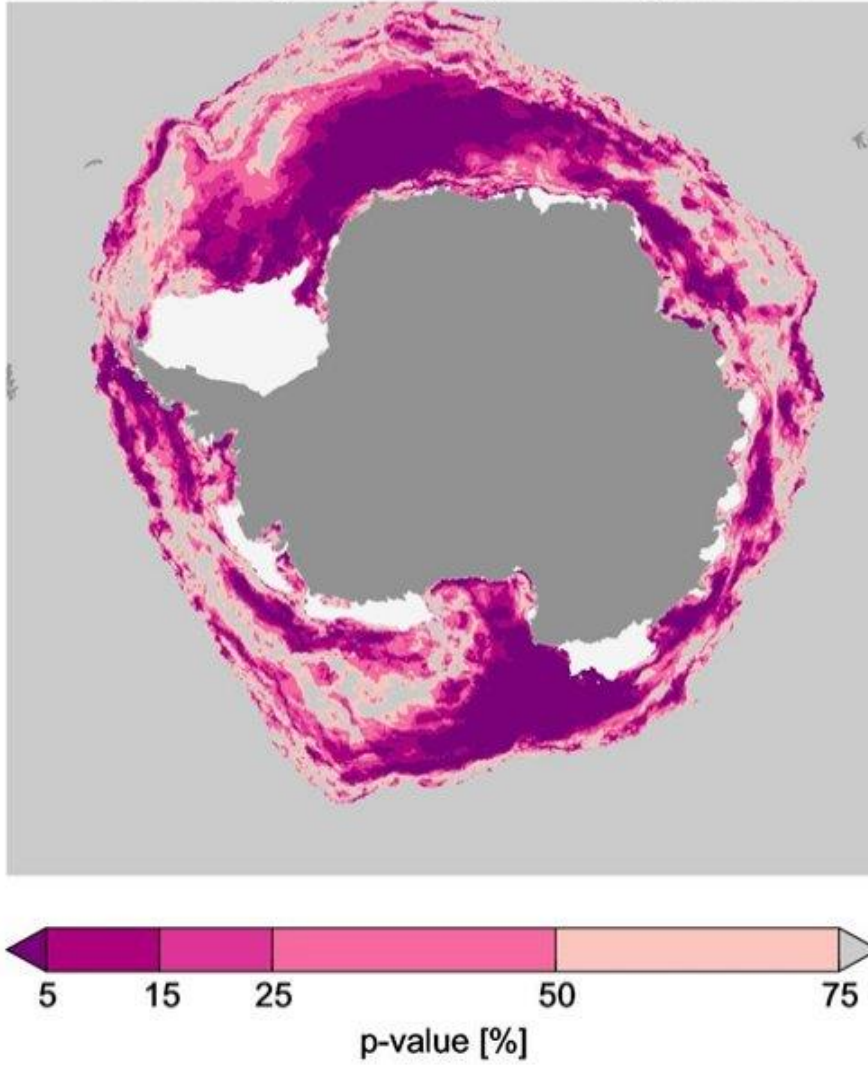


Figure 15. The probability that the trend in [figureFigure 14](#) is not significant (test of the null-hypothesis). A low value ($< 5\%$) indicates that the trend is in fact significant.

1
2
3
4
5
6

Formateret: Skriftype: 10 pkt

Formateret: Indrykning: Venstre: 0 cm, Mellemrum Efter: 0 pkt.